

Andreev - Saint James reflections: a probe of cuprate superconductors

Guy Deutscher*

School of Physics and Astronomy, Sackler Faculty of Exact Sciences Tel Aviv University, Ramat Aviv, Tel Aviv 69978, Israel

Electrical transport through a normal metal / superconductor contact at biases smaller than the energy gap can occur via the reflection of an electron as a hole of opposite wave vector. The same mechanism of electron-hole reflection gives rise to low energy states at the surface of unconventional superconductors having nodes in their order parameter. The occurrence of electron-hole reflections at normal metal / superconductor interfaces was predicted independently by Saint James and de Gennes and by Andreev, and their spectroscopic features discussed in detail by Saint James in the early sixties. They are generally called Andreev reflections but, for that reason, we call them Andreev - Saint James (ASJ) reflections. We present a historical review of ASJ reflections and spectroscopy in conventional superconductors, and review their application to the High T_c cuprates. The occurrence of ASJ reflections in all studied cuprates is well documented for a broad range of doping levels, implying that there is no large asymmetry between electrons and holes near the Fermi level in the superconducting state. In the underdoped regime, where the pseudo-gap phenomenon has been observed by other methods such as NMR, ARPES and Giaever tunneling, gap values obtained from ASJ spectroscopy are smaller than pseudo-gap values, indicating a lack of coherence in the pseudo-gap energy range. Low energy surface bound states have been observed in all studied hole doped cuprates, in agreement with a dominant d-wave symmetry order parameter. Results are mixed for electron doped cuprates. In overdoped $YBa_2Cu_3O_{7-\delta}$ ($\delta < 0.08$) and $La_{2-x}Sr_xCuO_4$, ASJ spectroscopy is consistent with the presence of an additional imaginary component of the order parameter. Results of ASJ spectroscopy under applied magnetic fields are also reviewed. A short section at the end is devoted to some recent results on spin effects.

arXiv:cond-mat/0409225v1 [cond-mat.supr-con] 9 Sep 2004

*Electronic address: guyde@tau.ac.il

Contents

I. INTRODUCTION	3
II. SOLUTION OF THE BdG EQUATIONS NEAR AN N/S INTERFACE	6
A. The case of a normal slab in contact with a semi-infinite superconductor	6
B. The case of a normal layer sandwiched between two superconductors. Effect of a phase difference.	7
C. Surface bound states in a d-wave superconductor	8
III. CONDUCTANCE CHARACTERISTICS OF SHARVIN CONTACTS	10
A. Sharvin contacts as a tool for ASJ spectroscopy	10
B. Fabrication of Sharvin contacts	11
C. BTK model	11
1. Case of a clean interface	11
2. Contacts with a finite transparency	12
D. HTSC Point Contact results for an anti-nodal orientation.	14
1. Early experiments on YBCO single crystal quality samples	14
2. Effect of the d-wave symmetry for an anti-nodal direction	14
E. Renormalization of the Fermi velocity	15
1. The problem of the small Fermi velocity mismatch	15
2. Solution to the problem	17
F. Concluding remarks	17
IV. ASJ SURFACE BOUND STATES	18
A. Zero Bias Conductance Peak and d-wave symmetry	18
1. KT results for the (110) orientation	18
2. KT results for arbitrary orientations	19
B. Experimental results	19
1. Low Z (110) contacts	19
2. High Z (110) contacts	21
3. High Z (110) contacts under magnetic fields	23
V. ASJ SPECTROSCOPY AND THE PSEUDO-GAP ISSUE	25
A. Manifestations and possible origins of the pseudogap	25
B. ASJ spectroscopy in the pseudogap regime	26
C. Compatibility of ASJ reflections and pseudogap models	28
1. RVB and other models emphasizing strong correlation effects.	28
2. The semiconductor-superconductor and strong coupling models	28
3. Two gap model	29
4. Some comments on the pseudogap	30
VI. SYMMETRY STUDIES AND SPIN EFFECTS	32
A. ASJ bound states under applied fields	32
B. Doping effect on the symmetry	32
C. Proximity effect on the symmetry	34
D. Spin effects	34
VII. CONCLUSIONS	36
Acknowledgments	36
References	37

I. INTRODUCTION

When an electron moving in a normal metal N with momentum k hits an interface with a superconductor S, it is reflected as a hole of equal momentum if its kinetic energy measured from the Fermi level is smaller than the energy gap Δ of S. Because of its negative effective mass, the reflected hole has a velocity opposite to that of the incoming electron, and carries charge current in the same direction. This process, known to day as an Andreev reflection (Andreev, 1964), was in fact first described by de Gennes and Saint James (De-Gennes and James, 1963) (and in a follow up paper by Saint James (Saint-James, 1964)) . The two independent original papers show solutions of the Bogoliubov -de Gennes equations (De-Gennes, 1966), based on the Bogolubov transformation (Bogoliubov, 1958), for the pair potential near an N/S interface. But they focus on different phenomena.

Andreev was interested in heat transport in the intermediate state of a Type I superconductor, and showed that domain walls provide a resistance to this flow because of the electron - hole reflection mechanism. This is why the thermal resistance in the intermediate state is higher than in the Meissner state, as observed by Mendelssohn and Olsen (Mendelssohn and Olsen, 1950). Andreev was able to fit quantitatively the detailed heat transport measurements of Zavaritskii (Zavaritskii, 1960). De Gennes and Saint James, on the other hand, were interested in the Density of States (DOS) in a system consisting of a normal slab of thickness d_N in close electrical contact with a semi-infinite superconductor. They showed that the DOS has a series of peaks below Δ because of the existence of finite energy bound states in N. For large enough values of d_N , these peaks are located at energies that are multiple of $(\hbar v_F/4d_N)$, where v_F is the Fermi velocity in N. Saint James (Saint-James, 1964) remarks that the inter-level distance is half of that for an electron in a potential well, and explains that this is because a complete cycle comprises two electron-hole reflections at the N/S interface and two specular reflections at the outer surface of N. In this cycle, the quasi-particle has both an electron like and a hole like character.

The Andreev 1963 paper was and still is widely quoted, may be because it explained a specific and observed physical phenomenon. The slightly earlier paper of de Gennes and Saint James (De-Gennes and James, 1963) is less quoted, and the slightly posterior paper of Saint James (Saint-James, 1964) is only known to some experts in the field. It is an excellent paper, whose reading I highly recommend. Its emphasis on the spectroscopic aspects of the electron-hole reflections is very close to our current interest, which will focus here on the use of these reflections for the spectroscopic study of High Temperature Superconductors (HTSC). After consulting with some colleagues, I decide for this reason to use in this review the terms of Andreev - Saint James (ASJ) reflections and spectroscopy.

Another curious aspect of the history of ASJ reflections is that it took almost 20 years before it was shown theoretically that they *enhance* the electrical conductance of N/S contacts at biases below the gap. This is in contrast with the *reduction* of the thermal conductance. This enhancement of the electrical conductance appears obvious to us to day. An electron coming in from the N side at energies smaller than Δ cannot propagate inside S, only Cooper pairs. The reflected hole ensures current conservation. A charge of $2e$ then flows across the interface, which corresponds to an increase of the conductance of the contact by a factor of 2 compared to that in the normal state, or at biases much larger than the gap. The detailed way in which the process occurs involves the creation of electron and hole excitations in S near the interface, which recombine into pairs over the coherence length of the superconductor. Pankove (Pankove, 1966) did report an enhanced electrical conductance of N/S contacts below the gap. His observations on pressure contacts between Al and Nb are clear: "When a contact is made between a normal metal and a superconductor, the V-I characteristic of the contact shows an initial region of high conductance with an abrupt change to a region of lower conductance". However, Pankove did not relate his observation to the works of Andreev and de Gennes and Saint James. Likewise, his observations were not noted by theorists. Griffin and Demers (Griffin and Demers, 1971) were the first to calculate the quasi-particle transmission probability for *excitations* going from a normal to a superconducting region for N/S contacts of various transparencies, but did not take into consideration the electron-hole reflection mechanism and the corresponding flow of *pairs*. It is not until 1980 that Zaitsev (Zaitsev, 1980) calculates an enhanced conductance below the gap, and only in 1982 Blonder, Tinkham and Kalpwijk (BTK) (Blonder *et al.*, 1982) give a complete theoretical discussion, including the effect of an imperfect (not fully transparent) interface, and successfully compare their predictions to measurements performed on Point Contacts.

Sharvin (Sharvin, 1965) had been the first to note that the electrical resistance of an ideal intermetallic contact of a size smaller than the electronic mean free path is determined by the number of quantum channels through the contact. These contacts, called Sharvin contacts or Point Contacts are the ideal tool for the study of ASJ reflections, for reasons that will be reviewed later in great detail. However, Sharvin apparently did not use them for that purpose, another strange twist in the history of ASJ reflections. Pankove contacts were actually Sharvin contacts, he calculates that their size is of about 50\AA , a typical Point contact contact size.

The transition between the region of higher conductance and that of lower conductance noted by Pankove occurs when the bias across the contact is equal to the energy gap. ASJ reflections are therefore a useful tool for the determination of the gap. BTK made this tool a quantitative one by taking into account a non ideal nature of the contact, including the effect of a thin insulating barrier and that of a mismatch of the Fermi velocities between the two

metals. Yet, their work had only a limited impact on the study of Low Temperature Superconductors (LTSC), may be because it came much later than the full development of tunneling theory (McMillan and J.M.Rowell, 1969) and also, I suppose, because the controlled fabrication of thin tunneling dielectric barriers had been achieved so successfully following the work of Giaever (Giaever, 1960).

By contrast, ASJ reflections have become a major tool for the study of unconventional superconductors, such as heavy fermions (Goll *et al.*, 1993; Hasselbach *et al.*, 1993), organic superconductors (see for instance (Ernst *et al.*, 1994)) and HTSC, which are the focus of this review. This development is the object of this review. One of the reasons why we became involved in this field was that we had strong doubts that dielectric junctions of a quality comparable to that achieved by Giaever on LTSC could ever be achieved on HTSC. Dielectric junctions made on LTSC are based on the oxidation of the metal. This method is not applicable to HTSC, because they are oxides by themselves, and further oxidation renders them even more metallic (and eventually non superconductors). Further, the fabrication of HTSC requires high temperatures of the order of 700 to 800 degrees Centigrade and the use of single crystal substrates, which precludes growing them on top of a regular metal previously oxidized. In our laboratory, we therefore decided to concentrate on the point contact route. In fact, observation of ASJ reflections turned out to be relatively easy. I believe that (Hass *et al.*, 1992) were the first to report such observations on single crystal quality YBCO samples, using a Gold tip as the normal metal. For reasons that became clear only later, and that had to do with the d-wave symmetry of the order parameter in this superconductor, the fit to BTK theory was not perfect, but a gap value of 18-20 meV could clearly be obtained. This value still stands to day.

However, a determination of the energy gap is not the only, and may be not the most important result of ASJ spectroscopy of HTSC materials. The following points will give the reader a preliminary idea of what the main results are:

a) A successful quantitative fit of point-contact data to the BTK theory, as has now been achieved in optimally doped samples, means that the BdG equations or in other words a Fermionic description of the excitations is appropriate for HTSC. ASJ reflections cannot occur without electron-hole mixing.

b) According to Blonder and Tinkham (Blonder and M.Tinkham, 1983), an enhanced conductance below the gap is only possible if the Fermi velocities of the normal tip and of the superconductor are not too different. That this should be the case in HTSC/ normal metal contacts is by no means trivial. In fact, Angle Resolved Photo Emission Spectroscopy (ARPES) data indicate for the HTSC a Fermi velocity of the order of $2 \cdot 10^7$ cm/sec (Margaritondo, 1998), almost one order of magnitude smaller than that of Gold. This apparent contradiction between experiment and theory was explained by Deutscher and Nozieres (Deutscher and Nozieres, 1994) as resulting from a renormalization of the Fermi velocity in the Point Contact experiments, which is different from the full quasi-particle renormalization. This special renormalization also explains the occurrence of strong ASJ reflections in heavy Fermions (Hasselbach *et al.*, 1993).

c) The BCS approximation of an energy gap that is very much smaller than the Fermi energy applies extremely well to LTSC, for which the gap value is typically less than 1 meV, and the Fermi energy value is of several eV. It applies only marginally to the HTSC at optimum doping, where the gap value is of a few 10 meV and the Fermi energy value a few 100 meV. It may not apply at all in underdoped samples, where a Bose Einstein condensation regime could be approached. The properties of ASJ reflections in a regime that is intermediate between BCS and Bose-Einstein condensation (Leggett, 1980; Nozieres and Schmitt-Rink, 1985) are a subject of great current interest. In particular, the existence of ASJ reflections in the presence of preformed pairs (or, more generally, of a pairing amplitude) without phase coherence is under intense consideration.

d) ASJ reflections are phase sensitive. This major difference with conventional Giaever tunneling spectroscopy turns out to be of great interest for the study of superconductors having an unconventional symmetry order parameter, as is the case for the HTSC. As shown by Hu (Hu, 1994), d-wave symmetry results in zero energy surface bound states, or ASJ bound states, when the orientation of the surface with respect to the crystallographic axis is such that there are interference effects between ASJ reflections from lobes of the order parameter of opposite signs. This is in contrast with the finite energy bound states calculated by de Gennes and Saint James. The case of p-wave superconductors had been earlier investigated by Buchholz and Zwicknagl (Buchholz and Zwicknagl, 1981).

This review is organized as follows. In Section II, I briefly present the original calculation of de Gennes and Saint James for a 1D situation giving the finite energy of bound states in a normal slab in contact with a superconductor, and contrast it with the zero energy states obtained in a hypothetical situation where the normal slab is sandwiched between two superconductors whose order parameters have phases that differ by π . This serves as an introduction to the effect of d-wave symmetry.

Section III is devoted to a brief summary of the BTK theory and to Point Contact experiments in geometries where the d-wave symmetry plays only a minor role. These experiments lead to determinations of the gap and of a Fermi velocity that is different from the fully renormalized value. Renormalization of the later as appropriate for point-contact spectroscopy is included in this Section. Effects related to the d-wave symmetry, and in particular the occurrence of surface bound states, are discussed in Section IV. This Section includes the effect of surface currents on

these states. Section V is devoted to ASJ reflections in the underdoped or so-called pseudogap regime, in relation to a possible BCS to Bose Einstein condensation crossover and other pseudogap models. Other advanced topics, such as the occurrence and detection of a minority imaginary component (*is* or *id*) of the order parameter and the proximity effect between HTSC and normal metals, are discussed in Section VI.

II. SOLUTION OF THE BDG EQUATIONS NEAR AN N/S INTERFACE

In order to make this review self-contained, we shall briefly outline here the main steps of the derivation that can be found in details in Saint James (Saint-James, 1964).

We consider two metals in ideal contact, the only difference between them being that one is a superconductor and the other a normal metal. We concentrate on quasi-particle excitations having an energy ε measured from the Fermi level smaller than the energy gap Δ . Such excitations will necessarily decay in S. They do so over a certain length scale, which turns out to be on the order of the coherence length ξ of the superconductor. At larger distances from the interface, all electrons are paired. Thus, the reflection process that we have briefly described in the introductory section, by which an electron coming from the N side is reflected as a hole, does not occur abruptly at the interface, but over the length scale ξ . This property, which appears explicitly in the calculation, will be of great importance when we discuss contacts with HTSC, in particular in the so called pseudogap region.

As it is, the calculation ignores the effect of the proximity of N on the value of the gap Δ in S near the interface. It is well known that this effect cannot in general be neglected and that a depression of Δ occurs over the length ξ (Deutscher and De-Gennes, 1969). However, in the actual Point Contact set up described by BTK (see next Section) the contact size is smaller than ξ , so that this depression effect is much reduced and can be neglected.

A. The case of a normal slab in contact with a semi-infinite superconductor

In a normal metal, the excitation energies of electrons and holes are derived respectively from the following relations:

$$\varepsilon u = [-(\hbar^2/2m)\nabla - E_F]u \quad (2.1)$$

$$\varepsilon v = [(\hbar^2/2m)\nabla + E_F]v \quad (2.2)$$

In a superconductor, excitations have a mixed electron-hole character and the above equations are complemented by crossed terms:

$$\varepsilon u = [-(\hbar^2/2m)\nabla - E_F]u + \Delta v \quad (2.3)$$

$$\varepsilon v = [(\hbar^2/2m)\nabla + E_F]v + \Delta^* u \quad (2.4)$$

The solutions for u and v are oscillatory in N, and for $\varepsilon < \Delta$ are decaying in S with complex wave vectors. The conditions at the interface, assuming that it is perfectly transparent, are that u and v and their derivatives are continuous. At the outer surface of N, assumed to be bonded by a dielectric, the boundary conditions are that u and v are zero. With the normal slab having a thickness d_N , and taking the origin at the interface, one dimensional solutions in N are of the form:

$$u = \alpha \sin[k'_1(x + d_N)] \quad (2.5)$$

$$v = \beta \sin[k'_2(x + d_N)] \quad (2.6)$$

with :

$$k'_1 = [(2m/\hbar^2)(E_F + \varepsilon)]^{1/2} \quad (2.7)$$

$$k'_2 = [(2m/\hbar^2)(E_F - \varepsilon)]^{1/2} \quad (2.8)$$

Solutions in S are of the form:

$$u = \alpha_1 \exp(ik_1 x) + \alpha_2 \exp(-ik_2 x) \quad (2.9)$$

$$v = \beta_1 \exp(ik_1 x) + \beta_2 \exp(-ik_2 x) \quad (2.10)$$

The wave vectors are given by:

$$k_1 = (2m/\hbar^2)^{1/2} [E_F + (\varepsilon^2 - \Delta^2)^{1/2}]^{1/2} \quad (2.11)$$

$$k_2 = (2m/\hbar^2)^{1/2} [E_F - (\varepsilon^2 - \Delta^2)^{1/2}]^{1/2} \quad (2.12)$$

Since we are interested in excitations for which $\varepsilon < \Delta$, these wave vectors are complex and their imaginary part ensures the exponential decay of the excitations inside S. We can write them in the form:

$$k_1 = K_1 + iK_2 \quad (2.13)$$

$$k_2 = K_1 - iK_2 \quad (2.14)$$

To a good approximation, $K_1 = k_F$, and $K_2 \ll K_1$. It is instructive to calculate explicitly the decay wave vector. To fix the order of magnitude, we easily obtain it for $\varepsilon = 0$:

$$K_2(\varepsilon = 0) = \Delta/\hbar v_F \quad (2.15)$$

Which, except for a factor of π is the inverse of the coherence length ξ . It is easily seen that the decay length diverges when ε approaches Δ .

The ratios (β_1/α_1) and (β_2/α_2) are determined by the BdG equations, so that there are 4 unknowns and 4 homogeneous linear equations relating them (the boundary conditions at the interface). After some simplifications resulting from the fact that $(\Delta/E_F) \ll 1$, the condition for the existence of a solution to the eigenvalue problem reads:

$$\tan(k'_2 d_N) = \tan(k'_1 d_N - \phi) \quad (2.16)$$

where ϕ is defined by:

$$\Delta \cos \phi = \varepsilon \quad (2.17)$$

Taking into account Eq.2.7 and 2.8, solutions of 2.16 are those of:

$$(2d_N/\pi\xi)\cos\phi = \phi + n\pi \quad (2.18)$$

where we have used the relation $\xi = (\hbar v_F/\pi\Delta)$. For any finite value of the normal slab thickness, there is no zero energy solution. An energy gap has been induced in N by the proximity with S. When the slab thickness is small compared to the coherence length, there is only one solution at $\varepsilon < \Delta$ and it approaches Δ . This bound state is in fact localized over the length ξ , over which excitations can penetrate inside S. When the thickness is much larger than ξ , ϕ , approaches $\pi/2$. There is a large number of solutions, the separation between the levels being:

$$\Delta\varepsilon = (\hbar^2/2m)(\pi k_F/d_N) \quad (2.19)$$

As noted by Saint James (Saint-James, 1964), this is half the spacing between the electronic levels in a 1D isolated normal metal of the same thickness. He explains this difference by noting that excitations in N in contact with S have a mixed electron-hole character. At energies smaller than Δ , the coefficients α and an β are close to each other. Over a complete cycle comprising two ASJ reflections at the N/S interface, and two specular reflections at the free surface of N, the quasi-particle is electron-like half of the time, and hole like the other half. This same Saint James cycle leads, as we shall see, to the formation of zero energy states at the surface of a d-wave superconductor.

In a more realistic 3D situation, instead of the discrete energy levels that we have obtained, the DOS is finite at any finite energy. Eigenvalues of the energy for quasi-particle trajectories making an angle Θ with the normal to the interface are reduced because the path traveled before the ASJ reflection takes place is longer. These eigenvalues tend to zero when Θ approaches $\pi/2$, but the solid angle covered by such trajectories tends itself to zero and as a result the DOS tends to zero linearly with ε (Fig.1).

B. The case of a normal layer sandwiched between two superconductors. Effect of a phase difference.

It follows from our analysis that we would have obtained the same eigenvalues if we had considered a normal slab of thickness $2d_N$ sandwiched between two superconductors. This is because in that case one reflection at each interface is sufficient to complete a cycle: an electron hitting the interface with S_1 is reflected as a hole, which is reflected back as an electron by S_2 . As a matter of fact, this geometry was used to study the proximity effect by thermal conductivity measurements of S/N/S sandwiches (Wolf, 1971). These measurements did reveal a reduced DOS in N. But for what concerns us here, the main interest of an S/N/S geometry is that it allows to look for the effect of a phase difference between the two superconductors on the DOS. Such a phase difference may for instance be induced by a current flowing perpendicular to the interfaces. To be specific, let us consider the case where this phase difference is equal to π (this will be the case of interest for a d-wave superconductor). The pair potentials in S_1 and S_2 have then opposite signs. The BdG equations impose that the ratios (u/v) will also have opposite signs in S_1 and S_2 . The continuity conditions at the interfaces then require that solutions in N will be of the form:

$$u = \alpha \sin[k'_1(x + d_N)] \quad (2.20)$$

$$v = \beta \cos[k'_2(x + d_N)] \quad (2.21)$$

The solution to the eigenvalue problem is then that of:

$$-\cot(k'_2 d_N) = \tan(k'_1 d_N - \phi) \quad (2.22)$$

$$(k'_2 d_N) - \pi/2 = (k'_1 d_N - \phi) + n\pi \quad (2.23)$$

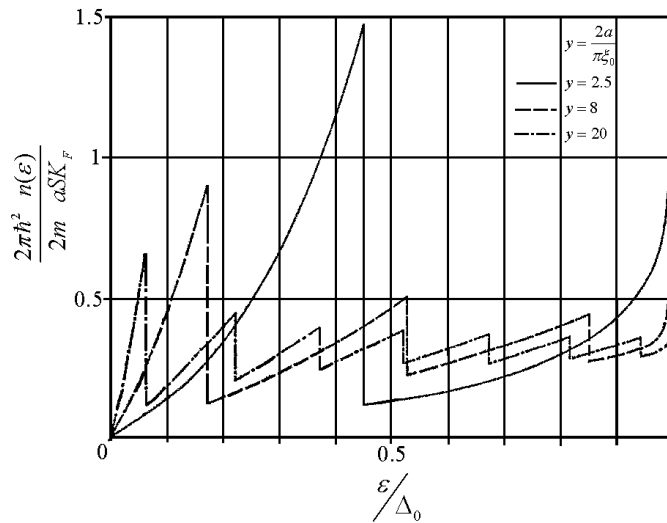


FIG. 1 Density of states for an N/S contact for different values of the normal layer thickness a . The thickness is given in terms of a normalized parameter $(2a/\pi\xi)$. (after Saint James 1964 op.cit.).

which gives the result:

$$(2d_N/\pi\xi)\cos\phi = \pi/2 - \phi + n\pi \quad (2.24)$$

Contrary to the case treated by Saint James, it is immediately seen that here $\phi = \pi/2$ is a solution for any value of the thickness. In other terms, there exists a solution with the eigenvalue $\varepsilon = 0$ even in the limit where the thickness of the normal slab is zero. In effect, one does not need a normal layer to obtain a zero energy bound state when there is a change of phase by π . This zero energy solution is localized near the interface between the two superconductors, it decays in the superconducting banks over a coherence length. It is a zero energy interface bound state. A self consistent solution would of course give a pair potential going to zero at the interface. The situation is similar to that near a vortex core: on opposite sides of the core, phase differ by π , the pair potential goes to zero at the center of the vortex core to accommodate this change in the phase, and there are low lying states of extension ξ (Caroli *et al.*, 1964).

C. Surface bound states in a d-wave superconductor

The situation described in the previous sub-section is somewhat artificial, particularly in the limit of a zero thickness normal slab. But this exercise helps understand what happens at the surface of a d-wave superconductor when it is oriented perpendicular to a node direction. For the $d_{x^2-y^2}$ symmetry, the pair potential is of the form:

$$\Delta = \Delta_0 \cos 2\theta \quad (2.25)$$

where θ is the angle with one of the principal axis. The pair potential is at a maximum along these axis, and changes signs at 45 degrees from them. The pair potentials on either side of these nodes have the same absolute values but opposite signs. Let us go back to the original Saint James geometry and consider a normal metal slab in contact with the surface of a d-wave superconductor having the above orientation (Fig.2). An electron in N moving towards the interface with a wave vector at some finite angle with the interface will be ASJ reflected as a hole by a pair potential having, say, the positive sign. This hole will then be specularly reflected at the outer surface of N, after which it will be ASJ reflected as an electron by a pair potential having the negative sign. This electron will then in turn be specularly reflected at the free surface of N, which will close the Saint James cycle. It is equivalent to that treated in the above sub-section: there are two successive ASJ reflections by pair potentials having phases that differ by π . Zero energy states are formed in N, and extend inside S over a coherence length. This geometry was first studied by Hu (Hu, 1994) who showed that zero energy states are formed even in the limit of a zero thickness normal slab, as in the above exercise. In the semi-classical approximation, they are zero energy surface bound states, or ASJ bound states.

The spectroscopy study of these states will constitute a substantial part of this review. Whenever detected they are a clear signature of a pair potential that reverses sign around the Fermi surface. They are modified by the presence of even a small imaginary component. such as is or id_{xy} , which cancels the sign reversal in the vicinity of a d-wave node.

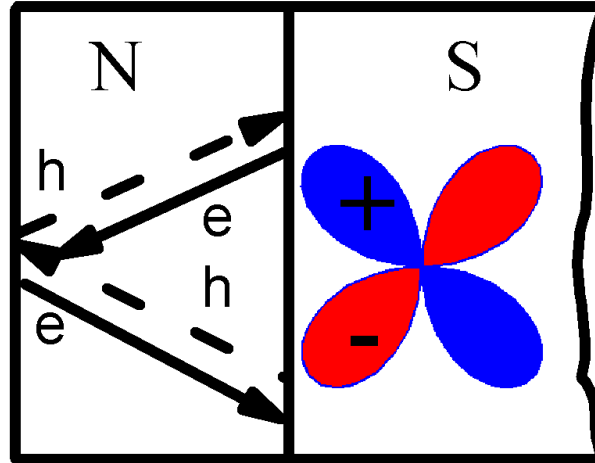


FIG. 2 Schematic representation of an ASJ cycle for a d-wave superconductor coated with a normal metal layer, the interface being oriented perpendicular to a nodal direction.

In this way, such components can be detected and their amplitude measured. In short, the spectroscopy study of ASJ states allows the determination of the detailed symmetry of the pair potential and that of the respective amplitudes of its components.

It will be appreciated that ASJ bound states will be best studied by tunneling from a normal metal electrode through a junction formed directly at the surface of the d-wave superconductor having the appropriate orientation. Making a clean contact with a normal metal would result in short lived ASJ states.

ASJ spectroscopy of the HTSC thus employs two different contact techniques: 1) clean Sharvin contacts are appropriate when formed on surfaces oriented perpendicular to an axis along which the order parameter is at its maximum, because in that geometry no ASJ bound states are formed and the amplitude of the gap is immediately accessible; 2) tunneling contacts are preferred when formed on surfaces oriented perpendicular to a (presumed) node direction, in order to detect the presence of ASJ bound states due to an unconventional order parameter symmetry. These two methods are reviewed in the following sections.

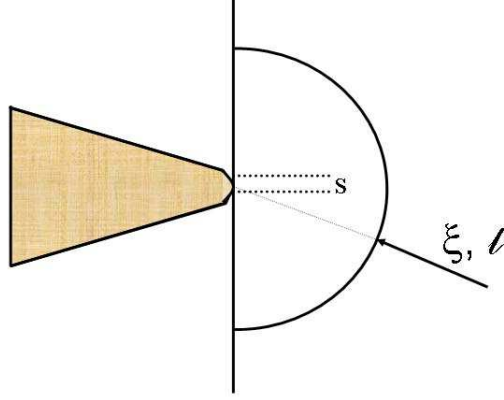


FIG. 3 Schematic representation of a Sharvin Point Contact having a size s much smaller than the coherence length ξ and the mean free path l . At biases of the order of the gap, the current density at the contact is of the order of the depairing value, but at distances of the order of (ξ, l) it is reduced much below that value. The condition $s \ll (\xi, l)$ avoids heating effects and quenching of superconductivity in the vicinity of the contact.

III. CONDUCTANCE CHARACTERISTICS OF SHARVIN CONTACTS

A. Sharvin contacts as a tool for ASJ spectroscopy

Let us consider a clean contact between two metals having a very small cross section a^2 , so that its electrical conductance in the normal state is equal to the number of quantum channels connecting them, multiplied by the quantum conductance (e^2/\hbar) . Namely, we neglect for the time being any resistance that might arise from a dielectric barrier between the two metals, or from a mismatch of the Fermi velocities between them. Such a situation can be nearly realized if we use broad conduction band metals since they all have Fermi velocities of the order of $1 \cdot 10^8$ cm/sec, and if we can avoid the formation of an oxide at the interface. The current voltage relationship of this contact is:

$$I = (e^2/h)(k_F a)^2 V \quad (3.1)$$

The current density through the contact is:

$$J = nev \quad (3.2)$$

where n is the carrier density and v their velocity across the contact. From 3.1 and the current density definition $J = (I/a^2)$, we obtain for the velocity the expression:

$$v = (eV/h)(k_F^2/n) \quad (3.3)$$

When we use Sharvin contacts to perform ASJ spectroscopy, the bias across the contact will reach values of the order of the pair potential. Using the value for the carrier density in the free electron model, we obtain at such bias a velocity of the order of:

$$v = (\Delta/p_F) \quad (3.4)$$

which is the depairing velocity in the superconducting side with gap Δ .

This high velocity is the main reason why we must use a contact size smaller than the electron mean free path in order to avoid heating effects, and also a contact size smaller than the coherence length (Fig.3). Spreading of the current after the contact bottleneck then reduces the current density below the depairing value already at distances smaller than ξ , thus avoiding quenching superconductivity at the contact, since superconductivity cannot be quenched over a length scale smaller than ξ .

In summary, a small contact size is favorable for three reasons: i) the condition $a \ll l$ makes the contact ballistic, which prevents heating effects at the large current densities reached at biases of the order of the gap; ii) the condition $a < \xi$ plays two roles: it prevents the weakening of superconductivity in S due to the proximity with N; and it prevents the destruction of superconductivity at biases of the order of the gap, where the carrier velocity reaches the depairing value (Δ/p_F) .

B. Fabrication of Sharvin contacts

In a clean superconductor the mean free path $l > \xi$, and the above conditions are met if $a < \xi$. In a LTSC, ξ is typically of the order of 1000\AA , and the contact qualifies as a Sharvin contact if $a \approx 100\text{\AA}$. For a HTSC, we would rather require $a \approx 10\text{\AA}$. When making a Point Contact, how can we make sure that such conditions are met?

The fabrication of point contacts has been well described in the literature, see for instance BTK (Blonder *et al.*, 1982). In short, a relatively sharp metallic tip, having a local radius of curvature of the order of 1 micron, is brought delicately in contact by a mechanical device with a bulk counter-electrode. The tip can be for instance made of a thin Gold wire, cut with a sharp razor blade. If the actual size of the contact were of the order of the radius of curvature of the tip, the above conditions would not be met. Its electrical resistance would be of the order of $1\text{m}\Omega$. In fact, the resistance of the contact is often found to be of the order of 10 to 100Ω . But how can we determine whether this larger value reflects actually a small contact size, or a dirty contact? We can get an answer to this question if we combine the value of the normal state resistance R_N (namely, its value above the critical temperature, or more practically its value well above the gap bias) with its value R_S at low bias (below the gap). In an ideal contact, we would have $(R_N/R_S) = 2$. This is of course never achieved. But a ratio $(R_N/R_S) > 1$, is an indication that ASJ reflections may dominate, although some junction structures (such as a proximity effect across the junction) may give such ratios and should be carefully checked for instance through the bias dependence of the conductance.

It turns out that in many cases the contact realized is indeed clean, and that its size falls in the range of a few 10\AA . One may wonder how that can happen, in view of the rather crude contact technique used here. The practitioners know from experience that when the tip is first brought in contact with the counter-electrode, the resistance is usually fairly high, in the range of a few $\text{k}\Omega$, and the $I(V)$ characteristic is structureless. By applying some slight movements to the tip, it is however possible to bring the resistance down to the interesting range of 10 to 100Ω , and to obtain meaningful characteristics. One may conjecture that these movements scratch away some of the insulating material at the surface, revealing the underlying pristine material. This, however, does not explain the very small size of the contact achieved. On the other hand, it is well known that when trying to produce a uniform tunneling barrier, one often encounters a problem of shorts presumably due to pinholes in the barrier. It may be that small good contacts are established through some naturally occurring defects in the insulating layer, but this is still imperfectly understood. Small size contacts have been observed using very different techniques of tip preparation, such as electro-chemical etching of a Nb wire, or cutting a thin Au wire with a sharp razor blade, as said before. A review of these methods of tip preparation can be found in Achsaf *et al.*, 1996.

C. BTK model

An electron moving from the N side towards the interface can be scattered in 4 different ways:

- i) it can be reflected as a hole along the incident trajectory (ASJ reflection) with probability $A(\varepsilon)$.
- ii) it can be reflected as an electron (normal specular reflection) with probability $B(\varepsilon)$.
- iii) it can be transmitted as an electron having a momentum $k > k_F$ (no branch crossing) with probability $C(\varepsilon)$.
- iv) it can be transmitted as an electron having a momentum $k < k_F$ (branch crossing) with probability $D(\varepsilon)$. The sum of these probabilities must be equal to one:

$$A(\varepsilon) + B(\varepsilon) + C(\varepsilon) + D(\varepsilon) = 1 \quad (3.5)$$

Since current is conserved across the interface, it suffices to calculate it for instance at the N side of the contact:

$$I = J_0 \int_{-\infty}^{+\infty} [1 + A(\varepsilon) - B(\varepsilon)][f(\varepsilon - eV) - f(\varepsilon)]d\varepsilon \quad (3.6)$$

where $f(\varepsilon)$ is the Fermi function and J_0 is a conductance taking into account the geometry of the contact.

BTK have given a complete calculation of the dependence of coefficients A and B on energy for barriers characterized by a *delta* function potential. For their derivation we refer the reader to their paper. Here below we limit ourselves to some simple limiting behaviors which we feel are of particular importance.

1. Case of a clean interface

For a clean interface, there are no specular reflections at the interface, $B(\varepsilon) = 0$. Also, $A(\varepsilon) = 1$ for $\varepsilon < \Delta$. For $\varepsilon > \Delta$, excitations can propagate in S. They have a partial electron character with amplitude u_o , and a partial hole

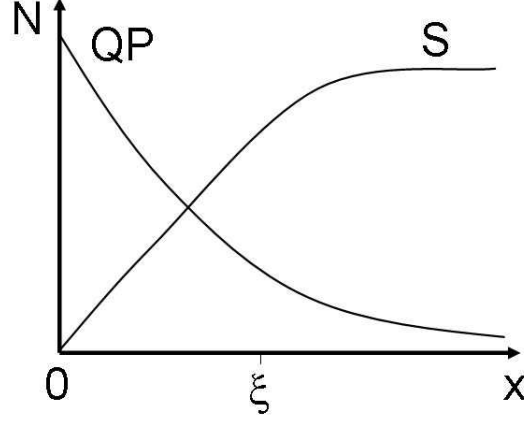


FIG. 4 Build up of the superfluid density S and decrease of the quasiparticle density QP in the S side of and N/S contact. ASJ reflections build up progressively over the distance ξ .

character with amplitude v_o . From BCS theory, we know that:

$$u_0^2 = [1 + (\varepsilon^2 - \Delta^2)^{1/2}/\varepsilon]/2 \quad (3.7)$$

$$v_0^2 = [1 - (\varepsilon^2 - \Delta^2)^{1/2}/\varepsilon]/2 \quad (3.8)$$

ASJ reflections occur in the proportion of the probabilities for hole to electron characters of the excitations propagating in S:

$$A(\varepsilon) = [1 - (\varepsilon^2 - \Delta^2)^{1/2}/\varepsilon]/[1 + (\varepsilon^2 - \Delta^2)^{1/2}/\varepsilon] \quad (3.9)$$

The conductance is equal to twice the normal state value below the gap, and goes back to it over a scale Δ in a manner that can be calculated from Eq.3.9 and Eq. 3.6.

It is interesting to consider more closely how the normal current in N is converted into a superfluid pair current in S (Fig.4). As already shown by Saint James, and noted earlier in this review, there are evanescent quasi-particle waves in S at excitation energies smaller than the gap. They decay over a length scale of the order of ξ , and are at the same time converted into superfluid. More precisely, BTK show that the decay length is given by:

$$\lambda = (\hbar v_F/2\Delta)[1 - (\varepsilon/\Delta)^2]^{-1/2} \quad (3.10)$$

This progressive conversion of quasi-particles into superfluid has important consequences, some of them we have already outlined. At a distance ξ from the interface, the current density is reduced by a factor $(a/\xi)^3$, which in a LTSC can be a factor of $1 \cdot 10^{-6}$. The velocity is then negligible compared to the depairing velocity even at biases much larger than the gap. The situation is evidently much less favorable in the HTSC because of their short coherence length. Then, we can hope at small bias to have at best $a \leq \xi$. However, as the bias is increased the situation becomes more favorable because of the divergence of the decay length. Another point, which is trivial for LTSC, is that propagation of quasi-particles over a distance ξ from the interface is necessary for the conversion to take place, and therefore for ASJ full reflections to occur. This condition is not a trivial one when we consider some situations peculiar to the HTSC, such as the existence of a pseudogap that may be larger than the pair potential. This special situation will be discussed in a later section.

2. Contacts with a finite transparency

BTK have calculated the coefficients $A(\varepsilon)$ and $B(\varepsilon)$ for contacts with a finite transparency which they have modeled with a δ function barrier $V = H\delta(x)$. They have used in their calculation a dimensionless parameter $Z = (H/\hbar v_F)$. For the case where the Fermi velocities in N and S are different, Blondeer and Tinkham (Blondeer and M.Tinkham, 1983) have shown that one can replace Z by an effective barrier parameter:

$$Z_{eff} = Z^2 + (1 - r)^2/4r^2 \quad (3.11)$$

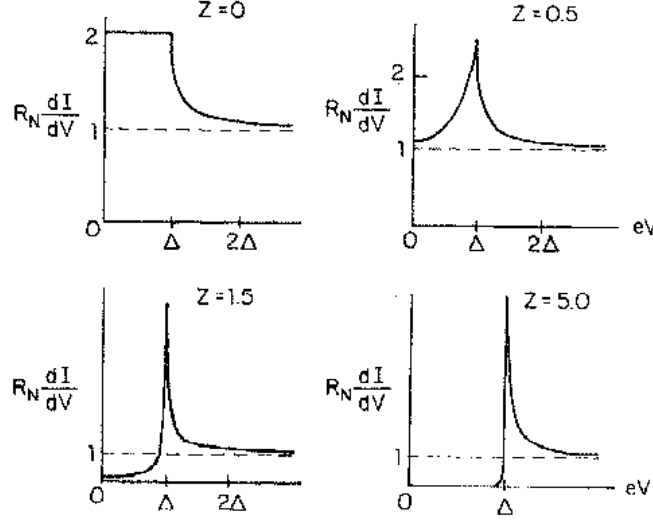


FIG. 5 Conductance characteristics of N/S contacts for various values of the barrier parameter Z (after Blonder *et al.* 1982).

Where $r = v_{FN}/v_{FS}$ (or the inverse). The shape of the $I(V)$ characteristics is a function of Z_{eff} only. There is no way one can distinguish between the effects of a dielectric barrier and that of a mismatch between the Fermi velocities. This result, obtained for a function barrier, is not general. In particular, it does not hold when the normal side is spin polarized (see the last section of this review).

A finite Z results in a finite probability of specular electron reflections at the N/S interface. $B(\varepsilon)$ is now finite, $A(\varepsilon) < 1$ even at $\varepsilon < \Delta$: the conductance below the gap is smaller than $2R_N^{-1}$, it goes to zero as Z is made very large. BTK have shown that at zero-bias:

$$A(0) = (1 + 2Z_{eff}^2)^{-2} \quad (3.12)$$

Since at biases smaller than the gap $C = D = 0$, it follows from the sum rule $A + B + C + D = 1$ and Eq.3.6 that the current at zero-bias is proportional to $2A(0)$. In the normal state, or at bias much larger than the gap, it is proportional to $(1 - B) = (1 + Z_{eff}^2)^{-1}$. From Eq.3.5 the ratio of the zero-bias to the high bias resistances, (R_S/R_N) is thus given by:

$$R_S/R_N = 2(1 + Z_{eff}^2)/(1 + 2Z_{eff}^2)^2 \quad (3.13)$$

From the measurement of the ratio of the contact resistances at high and zero-bias one can calculate the value of the effective barrier parameter. This value is useful for two purposes. First, it allows the calculation of the actual size of the contact by:

$$(k_F a)^2 = (h/R_N e^2)(1 + Z_{eff}^2) \quad (3.14)$$

Second, this parameter gives a lower bound to the ratio of the Fermi velocities by assuming the absence of any dielectric barrier at the interface.

More generally, using the analytical expressions derived by BTK for the coefficients $A(\varepsilon)$ and $B(\varepsilon)$, it is possible to fit experimental $I(V)$ curves and to extract values of the gap and of the barrier parameter. Fig.5 gives a few examples of conductance characteristics calculated for different values of the barrier parameter. As it increases, the normalized zero-bias conductance falls below 2, while at the gap edge it increases above 2. In fact, at the gap edge the conductance value is unaffected by the barrier. BTK have obtained values of the gap and of the Z parameter by fitting the conductance curves of Nb/Cu Sharvin contacts to the BTK theory (Blonder and M.Tinkham, 1983). Characteristics could be fitted successfully for normal state resistances falling in the range of 10 to 100Ω. Reported values of Z_{eff} are smaller than 1, and can be as small as 0.3. Calculated contact radii vary from 10 to 120Å, fully qualifying them as Sharvin contacts meeting the conditions $a < (\xi, l)$. The bound to the mismatch of the Fermi velocities is as expected. In fact, the experimentally determined values of the effective barrier parameter mean that the contact is basically a clean one. In turns, this justifies modeling the barrier as a δ function, since the mismatch of the Fermi velocities occurs over an atomic distance.

D. HTSC Point Contact results for an anti-nodal orientation.

1. Early experiments on YBCO single crystal quality samples

The earlier Sharvin point-contact experiments on single crystal quality samples were performed by Hass *et al.* (Hass *et al.*, 1992) on melt textured YBCO samples cut out in a cubic shape so that four faces had the (100) or equivalent orientation, and two the (001) orientation. As already noted, the main motivation for attempting this experiment was the hope that there was a better chance to obtain a good point contact than to make a good tunnel junction. They revealed the following main features:

- on (100) faces, contacts with a normal state resistance of about 10Ω could be made. Their conductance increased by about 50% below a bias of about 20 mV (Fig.6). This bias value was interpreted as being the gap edge. The shape of the characteristic was generally in accordance with the predictions of BTK for a barrier parameter of about 0.3, except for two features. First, the return to the normal state conductance above the gap was somewhat faster than it should have been; this might have been due to the fact that the condition $a < \xi$ was only barely met, because of the short coherence length. Second, the data did not show the expected conductance peak at the gap edge. The absence of this conductance peak was also noted later on similar contacts produced on LSCO samples (Hass *et al.*, 1994). The main surprise came from the substantial enhancement of the conductance at low bias, which implied a small mismatch of the Fermi velocities.

- on (001) oriented faces, the characteristics were basically structureless except for an occasional zero-bias peak, and positive slopes at negative as well as positive biases. The absence of a conductance enhancement at low bias for this orientation was expected, in view of the large mismatch of the Fermi velocities for that case. However, BTK theory then predicts that the characteristic should have the shape of a regular Giaever tunneling junction, which was not observed.

2. Effect of the d-wave symmetry for an anti-nodal direction

The original theory of BTK is not appropriate for d-wave symmetry. However, the later does not have dramatic effects for an anti-nodal direction, probed in the experiments of Hass *et al.* (Hass *et al.*, 1992). As noted above, there are no ASJ low energy surface bound states for that orientation, because specular reflections at the surface then preserve the value and the sign of the pair potential. The coefficients A and B can be calculated by performing a 2D integral of the BTK coefficients over all angles. For clean contacts, having an effective Z parameter smaller than 1, it is not necessary to take into account a finite tunneling cone aperture. Typical conductance characteristic shapes are shown Fig.(7) (Z values: 0; 0.2; 0.3; 0.5; 0.7; 1.0). For $Z = 0$, they assume a triangular shape; for Z values around 0.3, they are rather flat up to the gap edge, this is the case observed in the early experiments on YBCO shown above; for Z values in the range of 0.5 to 1, they assume a V shape at low bias, reaching a maximum slightly below the gap, followed by a sharp descent back to the normal state conductance. It is noticeable that for an anti-nodal direction, in this range of Z values which is typical for Point Contacts, the maximum conductance reached is always smaller than twice the normal state value. Typical maximum conductance values are around 30 to 50% higher than the normal state value.

The d-wave symmetry explains the main disagreement between the data of Hass *et al.* (Hass *et al.*, 1992) and the original BTK theory, namely a conductance at the gap edge smaller than twice the normal state value. Actually, the various theoretical shapes calculated for the range $0 < Z < 1$ have been observed experimentally. Fig.(8) shows data obtained on an a-axis oriented YBCO surface (Kohen *et al.*, 2003) and Fig.(9) data obtained on a BiSrCaCuO single crystal in the (100) orientation (D'Gorno and Kohen, 1998), with fits to theory. The predicted V-shape at low bias is clearly observed in both cases. Fits are of a high quality, and require only a small "smearing" factor Γ (Kohen *et al.*, 2003). They establish that ASJ spectroscopy is a reliable and quantitative spectroscopic tool for the study of HTSCs. When performed in an anti-nodal direction, it provides a precise determination of the gap value. The effect of the d-wave symmetry is also clearly seen in the shape of the characteristics.

Two kinds of deviation from pure d-wave behavior have been reported. A special proximity effect has been observed between the normal tip and the d-wave superconductor at very small Z values ($Z < 0.5$), which may induce an s component in the superconductor. This is discussed in detail in the last section of this review. Another deviation has been seen in strongly overdoped YBCO samples. It involves a small imaginary minority component (id_{xy} or is), whose occurrence is also discussed in the last section.

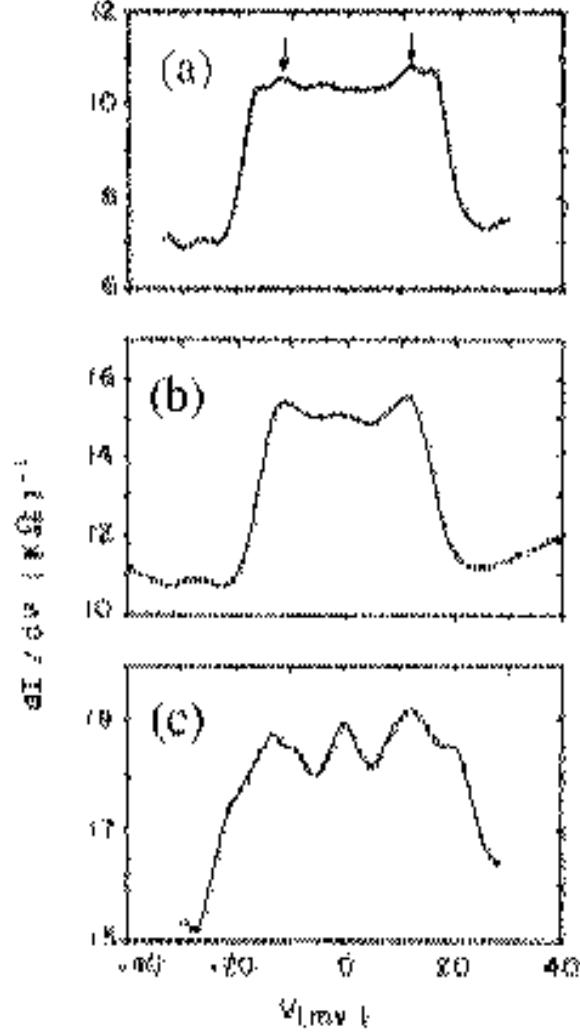


FIG. 6 Conductance characteristics of Au/YBCO Point Contacts for the anti-nodal orientation (after Hass *et al.* 1992). The increase of the conductance at low bias is of about 50%. The edge is at about 20 mV. Note the absence of a conductance peak at the gap edge. Data from three different locations on the same sample.

E. Renormalization of the Fermi velocity

1. The problem of the small Fermi velocity mismatch

The other question raised by the experiments of Hass *et al.* was the surprisingly small value of the barrier parameter needed to fit some of the data. Z values of 0.3 to 0.4, as found for YBCO (Hass *et al.*, 1992; Wei *et al.*, 1998) imply that the ratio between the Fermi velocities of YBCO and of the normal tip is at most a factor of 2 (assuming that the finite Z is entirely due to the Fermi velocity mismatch). Taking for instance the case of the Au tip, where the Fermi velocity is $1.4 \cdot 10^8$ cm/sec, one obtains for the Fermi velocity in YBCO a lower bound of $0.7 \cdot 10^7$ cm/sec. This is more than three times larger than the velocity measured by ARPES in BiSrCaCuO, $v_{FS} = 2 \cdot 10^7$ cm/sec (see for instance (Margaritondo, 1998)), which is presumably typical of all HTSC. Using this value of v_{FS} , one obtains $Z = 6$. For such a high Z value, the point-contact characteristic should be a tunneling one (Tanaka, 1996), namely the small bias conductance should be much smaller than the normal state value, contrary to what is observed experimentally.

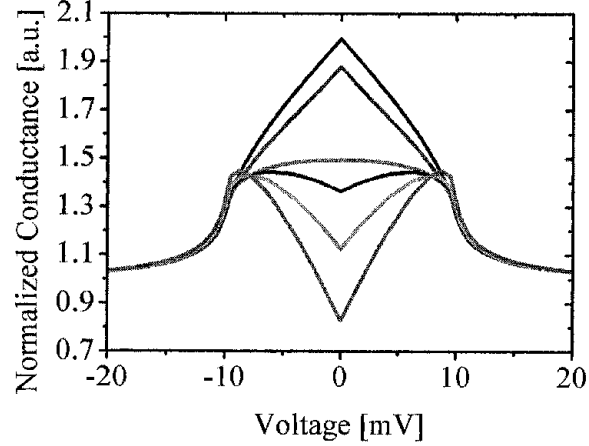


FIG. 7 Calculated conductance characteristics for a d-wave order parameter in an anti-nodal orientation, at different values of the barrier parameter Z (0; 0.2; 0.3; 0.5; 0.7; 1.0). Note for $Z > 0.5$ the clear V-shape at low bias and the sharp decrease of the conductance at the gap edge.

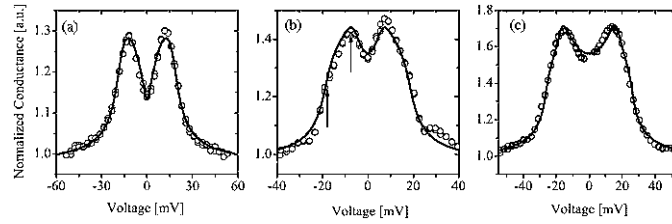


FIG. 8 Conductance characteristics of Au/YBCO films contacts fitted to a d-wave order parameter for different values of the barrier parameter Z (from left to right: 0.68; 0.49; 0.34). The fit is for an anti-nodal direction. Note the well pronounced V-shape at low bias for the highest Z contact. (after Kohen *et al.* 2003).

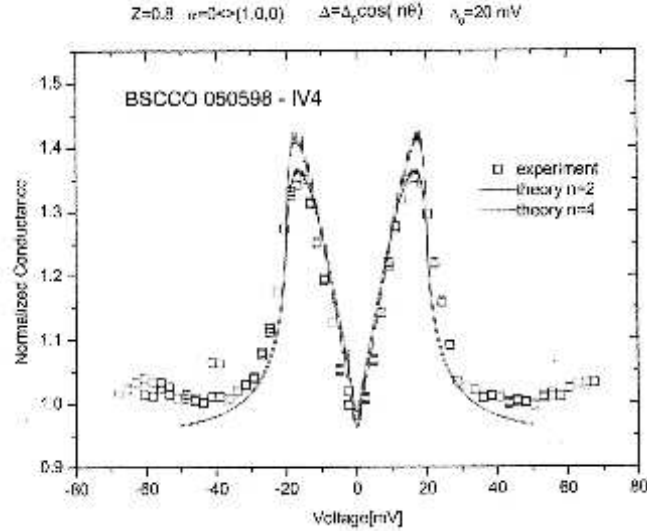


FIG. 9 Measured conductance characteristic of a $Au/Bi_2Sr_2CaCu_2O_8$ in-plane contact to a bulk oriented sample. Note the low bias V-shape and the sharp drop at about 20 mV. The fit is for an anti-nodal direction and $Z = 0.8$. (After I. Okashi and A. Kohen privet communication)

2. Solution to the problem

As shown by Deutscher and Noziers (Deutscher and Noziers, 1994), the solution to the problem lies in the fact that the small value of the quasi-particle Fermi velocity in the cuprates is a many body effect, which does not come into play in the mismatch that governs ASJ reflections. The quasi-particle velocity is:

$$v_F = z\bar{v}_F \quad (3.15)$$

where:

$$\bar{v}_F = v_{F0} - \partial\Sigma/\partial k \quad (3.16)$$

and:

$$z = 1/(1 + \partial\Sigma/\partial\omega) \quad (3.17)$$

v_{F0} is the bare Fermi velocity (the band velocity, undressed for interaction effects), Σ is the self-energy correction $\Sigma(k, \omega)$. The wave vector dependence of the self energy is a non-local effect (usually quite small in metals), and its energy dependence is a retardation effect, leading to mass enhancement. This factor can sometimes be extremely large, like in heavy fermions (Hasselbach *et al.*, 1993). It is in principle accessible by a measurement of the low temperature electronic heat capacity. In practice, however, that is not possible in the high- T_c cuprates, because of their extremely high critical field. Another quantity that is sensitive to the mass enhancement factor is the coherence length, since it is the quasi-particle velocity that enters into that length:

$$\xi = \hbar v_F / \pi \Delta \quad (3.18)$$

where Δ is the measured gap. We can obtain the value of v_F from Eq.3.17, putting in the value of ξ derived from the measured upper critical field $H_{c2} = \phi_o/2\pi\xi^2$, and the value of Δ obtained for instance from ASJ spectroscopy, as described in the previous paragraph. We can then calculate the mass enhancement factor z by comparing this value of v_F to the lower bound of the velocity obtained from the effective barrier parameter Z_{eff} determined from a fit to point-contact conductance characteristics.

If we take the specific example of YBCO, from $\xi = 15\text{\AA}$, $\Delta = 20$ meV, we calculate for the quasi-particle velocity $v_F = 1.510^7$ cm/sec. The lower bound of the velocity obtained from the lowest measured $Z_{eff} = 0.3$ is, from Hass *et al.* 1992, 6 to $7 \cdot 10^7$ cm/sec, giving a mass enhancement factor of 4 to 5. It should be emphasized that this factor combines two effects: non-locality and retardation. The respective contributions of these two effects cannot be determined directly. This would require a fairly exact knowledge of the bare band velocity. From Massida *et al.* (Massida *et al.*, 1991) it is smaller than the velocity derived from the point-contact measurements, suggesting that both contributions are important.

F. Concluding remarks

In this Section, we have reviewed the application of the BTK model to the study of ASJ reflections. We have shown that it can be applied successfully, in a quantitative way, to point-contact experiments carried on HTSC in configurations where phase effects due to the d-wave symmetry of the order parameter are not dominant. The BTK model is based on a solution of the Bogoliubov - de Gennes equations for the pair potential. Use of these equations assumes implicitly a Fermi liquid description of the HTSC. The high quality of the fits between experiment and theory shows that this assumption is justified, at least for samples near optimum doping. The exact shape of the point-contact conductance characteristics obtained on surfaces perpendicular to an anti-nodal direction is in excellent agreement with a d-wave order parameter. The small value of the barrier parameter Z implies a good match between the Fermi velocities of the normal metal tip and the HTSC, which is well explained by a mass enhancement effect in the spirit of Fermi liquid theory.

Geometries where the d-wave symmetry has a more dramatic effect are reviewed in the next section.

IV. ASJ SURFACE BOUND STATES

As briefly introduced in II.C, zero energy ASJ surface bound states are a direct result of a d-wave symmetry of the order parameter when the surface is oriented perpendicular to a nodal direction ((1,1,0) oriented surface). The origin of these states lies in the sign reversal of the pair potential "seen" by quasi-particles upon specular reflection at the surface. For reasons of symmetry, sign reversal for this orientation will occur for trajectories making any angle with the normal to the surface. For other surface orientations, sign reversal will occur for a certain angular range, with the exception of the case of the anti-nodal orientation, reviewed in IIID, where there is no sign reversal for any trajectory. Hence, zero energy surface bound states will exist for any surface orientation, except for the anti-nodal one. In the (more practical) case of diffuse reflections at the surface, for any orientation of the surface there will always be a sign reversal for some trajectories. Surface bound states are therefore a robust property of d-wave superconductivity.

A. Zero Bias Conductance Peak and d-wave symmetry

Motivated by the findings of Hu (Hu, 1994), Kashiwaya and Tanaka (KT) (Kashiwaya *et al.*, 1995) have extended the model of BTK to the case of a d-wave symmetry, for all surface orientations.

The main difference with the results of BTK, obtained for the s-wave symmetry case, comes about when one considers the two transmission channels having the respective transmissions probabilities $C(\varepsilon)$, for an electron-like transmission, and $D(\varepsilon)$ for a hole like transmission. While in the s-wave case a 1D calculation was sufficient, automatically taking care of momentum conservation in the direction parallel to the interface, here a 2D calculation is necessary.

1. KT results for the (110) orientation

We summarize here KT's results for the nodal orientation. We follow KT's notation and define a normalized conductance:

$$\sigma(\varepsilon) = \bar{\sigma}_S(\varepsilon)/\bar{\sigma}_N(\varepsilon) \quad (4.1)$$

where:

$$\bar{\sigma}_i(\varepsilon) = \int_{-\pi/2}^{+\pi/2} \bar{\sigma}_i(\varepsilon, \phi) d\phi, (i = N, S) \quad (4.2)$$

ϕ being the angle with the normal to the surface.

In the limit $Z \gg 1$, KT's expressions reduce to:

$$\bar{\sigma}_N(\varepsilon, \phi) = 4\cos^2\phi/Z^2 \quad (4.3)$$

$$\bar{\sigma}_S(\varepsilon, \phi) = 32\cos^4\phi/|4\cos^2\phi + Z^2(1 + \Gamma^2)|^2 \quad (4.4)$$

with:

$$\Gamma = \varepsilon/|\Delta| - [(\varepsilon/\Delta)^2 - 1]^{1/2} \quad (4.5)$$

At zero-bias, we have just $\sigma_S(0, \phi) = 2$. The conductance is twice as large as the value it would have *in the normal state in the absence of any barrier* (Deutscher and Maynard, 1998). On the other hand, the actual normal state conductance varies as Z^{-2} . Hence the appearance in the measured conductance of what is called a Zero Bias Conductance Peak, or ZBCP, for a high barrier contact. The bias range over which the conductance is substantially enhanced compared to its actual normal state value is:

$$|\varepsilon/\Delta| \leq Z^{-2} \quad (4.6)$$

As the barrier height is increased, the conductance peak becomes higher and narrower. Life time effects and discrete lattice effects on the ZBCP have been discussed by Walker and Pairor (Walker and Pairor, 1999). They broaden and reduce the ZBCP. Discrete lattice effects limit zero energy bound states to certain orientations of the wave vector. They can also modify the shape of the ZBCP near zero-bias. There can thus be substantial deviations from the KT

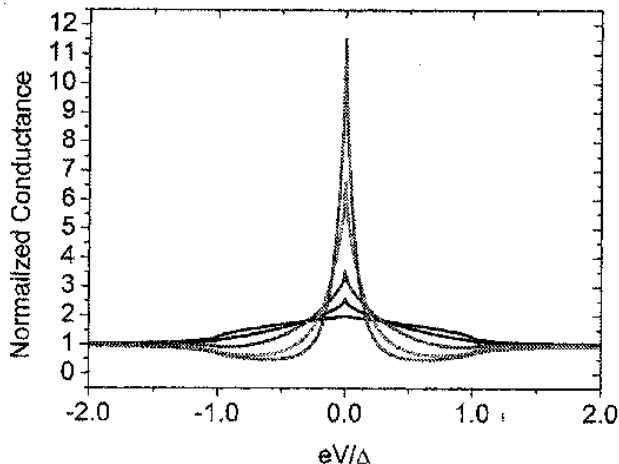


FIG. 10 Calculated conductance characteristics for a contact to a d-wave superconductor in a nodal direction, for different values of the barrier parameter Z (0; 0.5; 1.0; 2.0; 3.0). Contrary to the case of anti-nodal contacts, there is no sharp structure at the gap bias, only a smooth return to the normal state conductance.

expressions. Since the conductance at zero-bias $G_S(0)$ is unaffected by the presence of a barrier for a pure (110) orientation, its value may be used to calculate the actual size of the contact:

$$(k_F a)^2 = (\hbar/e^2)G_S(0) \quad (4.7)$$

Fig.(10) shows how the shape of the conductance characteristic evolves as a function of Z for the (110) orientation. For $Z = 0$, it has a triangular form, the conductance at zero-bias being twice as large as the normal state value, reached when the applied bias is equal to the value of the gap. For $Z \gg 1$, the conductance dips below its normal state value before returning to it at a bias of the order of the gap. Notice that the gap is not marked by a sharp structure at any value of Z . Hence, the (110) orientation is not as favorable as the (100) one for an accurate determination of the gap. On the other hand, it is highly sensitive to the symmetry of the order parameter.

2. KT results for arbitrary orientations

KT (Kashiwaya *et al.*, 1995) have given expressions for the amplitudes of holes $a(\varepsilon, \phi)$ and electrons $b(\varepsilon, \phi)$ reflections. These expressions allow to calculate the I(V) characteristics for any surface orientation and Z value, taking into account a possible angular dependence of Z in the case of a strong barrier (tunneling cone). The ZBCP is a robust feature of the d-wave symmetry (Fig.11) (Yang and Hu, 1994). It occurs for any orientation of the surface, except the (100) one, and for any value of Z . The structure at the gap edge is in general a weak one. It can be a small step down at low Z values, or a small step up at large Z values, or a weak maximum at large Z values and intermediate orientations. An important difference with a contact to an s-wave superconductor is that no large conductance peak is predicted at the gap edge (even for the (100) orientation it remains of modest height). This peak, called the coherence peak in s-wave superconductors, is destroyed for in-plane tunneling by the very interference effects that give rise to the ZBCP.

B. Experimental results

We review successively results obtained for low Z contacts (Sharvin contacts) and high Z contacts (tunneling contacts).

1. Low Z (110) contacts

Fig.(12) shows the conductance of a contact prepared on a (110) face of a LSCO single crystal (Dagan *et al.*, 2000). The crystal itself had $T_c = 33\text{K}$, near optimum doping, but the local T_c at the contact was only 16K, probably due

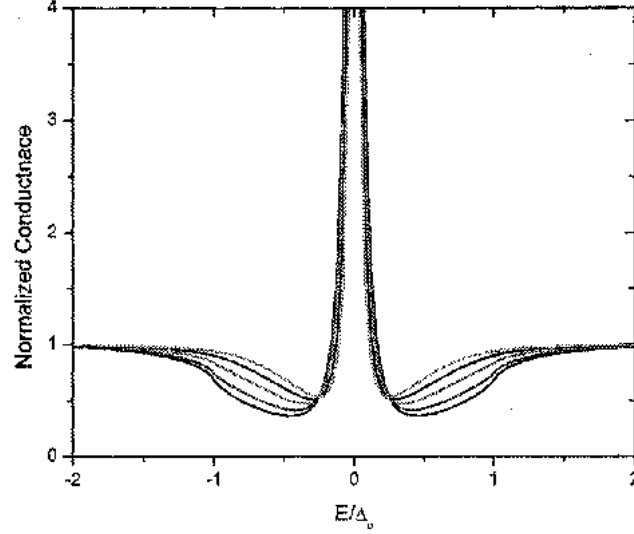


FIG. 11 Calculated conductance characteristics for a contact to a d-wave superconductor in a nodal direction with $Z = 5$, at different openings of the tunneling cone. Return to the normal state conductance always occurs at about the gap value. The curves have been calculated using the weight function $\exp[-(\theta/\theta_M)^2]$, with θ_M values 90, 57, 33, 23, 18 degrees.

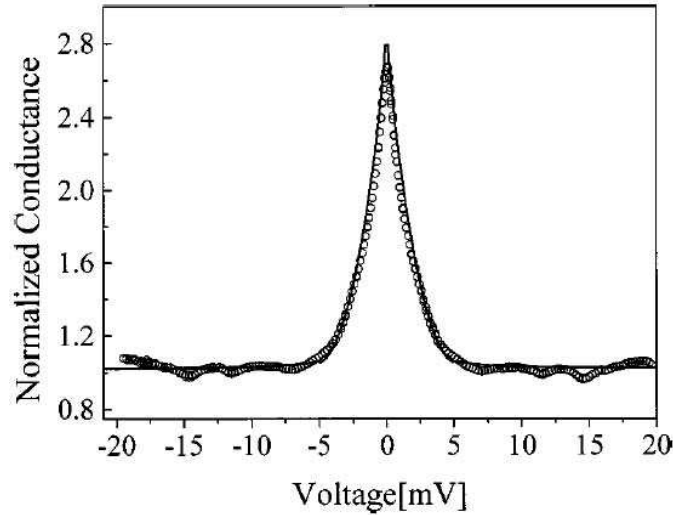


FIG. 12 Measured conductance characteristic of a $Au/La_{2-x}Sr_xCuO_4$ single crystal underdoped contact. The data was fitted for a nodal direction, giving $Z = 0.3$, and a gap of 5 meV (after Dagan *et al.* 2000).

to the manipulations used to prepare it, resulting in a local loss of oxygen. The characteristic has the shape of an inverted V, in agreement with the theoretical predictions for a low Z (110) surface (Fig.7). A fit to theory gives $\Delta = 5$ meV. This result will be important when we discuss the underdoped regime (pseudogap regime) in the next section.

Low Z contacts on LSCO at actual optimum doping have slightly different characteristics. Fig.(13) shows that of a contact obtained by electro-migration (Achsaf *et al.*, 1996). Upon making contact between the tip and the sample, the resistance was first very high, in the 100k Ω range, presumably due to an oxygen depleted surface layer. A positive bias was then applied to the tip, possibly attracting positively charged oxygen ions from the bulk of the sample towards the surface. The general shape of the characteristic is still that of an inverted V, but with a local minimum near zero-bias. As explained in the theory section, this local minimum is incompatible with a pure d-wave symmetry.

Etching the surface is another way to obtain a low Z contact. On the same crystal, this method lent characteristics having the same general shape as that obtained on a junction prepared by electro-migration, shown above, but with a wider separation between the two peaks. It may be that etching exposes other crystallographic facets besides (110), giving a characteristic more similar to that obtained on (100) surfaces. Similar characteristics were obtained by

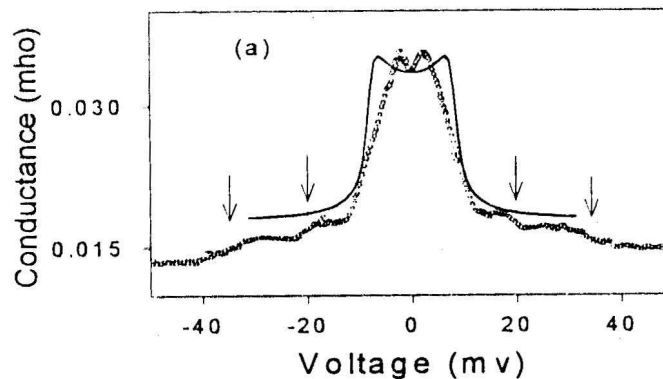


FIG. 13 Measured conductance characteristic of a $Au/La_{2-x}Sr_xCuO_4$ single crystal contact near optimum doping. Note the small split of the conductance peak at small bias. The line is an attempt to fit the data with an s-wave gap. Arrows indicate high bias structures possibly related to phonons. (after Achsaf *et al.* 1996)

Gonelli *et al.* (Daghero *et al.*, 2002) on polycrystalline LSCO samples. They were also interpreted as indicating a mixed symmetry.

Concerning the gap value, Achsaf *et al.* (Achsaf *et al.*, 1996) conclude from their low Z data that it is of about 9 meV in a slightly underdoped LSCO single crystal. This is somewhat smaller than the value of the gap obtained from tunneling contacts on the same crystal, which is closer to 15 meV.

Relatively low Z contacts ($Z = 1$) were obtained by Wei *et al.* (Wei *et al.*, 1998) on an optimally doped YBCO single crystal by driving a Pt-Ir tip into the sample. The characteristics had also the shape of an inverted V. The gap value extracted from the fit is 27 ± 4 meV. For comparison, a regular STM measurement taken along the c-axis on the same crystal gives a gap value of 19 ± 4 meV.

2. High Z (110) contacts

In agreement with theory, high Z contacts to (110) oriented surfaces show a ZBCP and a weak structure at the gap edge.

Sinha and Ng (Sinha and Ng, 1998) have produced tunnel junctions on the edges of BSCCO single crystals by evaporating onto them a Pb or a Ag counter-electrode. The roughness of the edge is large (3000\AA), therefore there is no well defined surface orientation. Taking this orientation as a free fit parameter, and a smearing factor of 3.08 meV Sinha et Ng obtained a good fit of their data to KT theory, with $Z = 2$ and $\Delta = 13$ meV. One can see from Fig.(14) that the zero-bias conductance is larger than the normal state conductance by a factor larger than two, and that the gap edge has a weak signature as a dip below the normal (high bias) conductance value followed by a progressive recovery. The T_c of the junction was 75K, presumably indicating underdoping at the surface, either intrinsic or provoked by the contact with the counter-electrode. The rather small gap value will be commented upon in relation with the pseudogap issue in the next section.

Wei *et al.* (Wei *et al.*, 1998) measured the characteristics of STM tunnel junctions on (110) faces of an YBCO single crystal. They show a large ZBCP, the conductance at zero-bias reaching up to 8 times the normal state value. As predicted by theory, the peak is followed by a dip before return to the normal state (high bias) value. The gap value obtained from the fit is 27 ± 4 meV.

In general, the highest ZBCPs have been obtained on STM junctions. STM reveals neatly the large anisotropy in the TDOS of the HTSC. Sharoni *et al.* (Sharoni *et al.*, 2001) have reported observing on the same sample, a c-axis oriented YBCO film, three types of characteristics: respectively V-shaped on (001) areas, ZBCP dominated on (110) edges and flat bottom on (100) edges (Fig.15) (see also Sharoni *et al.* 2003). These observations show that the TDOS can vary over a length scale of the order of the nanometer. On (110) oriented films, a ZBCP and a Gap Like Feature (GLF) are both observed (Sharoni *et al.*, 2002). Macroscopic contacts allowing in-plane tunneling into films having the (100) or (110) orientations have been produced by a number of techniques such as: using a Pb counter-electrode (sometimes with a thin Ag buffer layer in order to avoid massive oxygen out-diffusion, Lesueur *et al.* 1992); or a copper counter electrode (Aprili *et al.*, 1999). The method that we have been mostly using is sticking a small In dot on the film's fresh surface (Krupke and Deutscher, 1999). These contacts are very stable and can sustain repeated thermal cycling without damage. The exact nature of the dielectric layer is not known. It can be the result of some loss of oxygen at the surface, resulting in an underdoped YBCO insulating surface; or to oxidation of the In counter-electrode

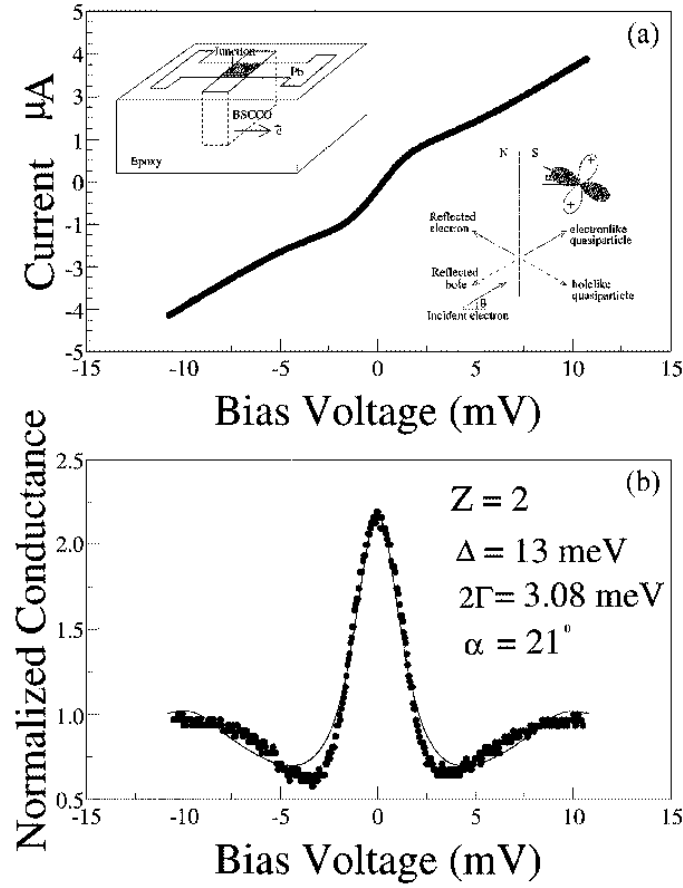


FIG. 14 $I(V)$ and conductance characteristics of an in-plane contact to a $\text{Bi}_2\text{Sr}_2\text{CaCu}_2\text{O}_8$ single crystal. Note the return to the normal state conductance at about 10 meV (after Sinha and Ng 1998).

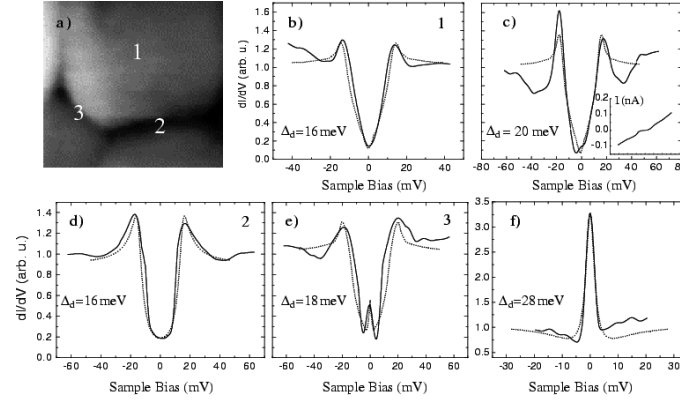


FIG. 15 Measured STM conductances at various positions on an YBCO grain having a (001) oriented upper surface. The shape of the characteristics goes from V-shape on top of the grain (b,c), to U shape near a (100) face (d), to inverted V near a (110) face (e,f) (after Sharoni *et al.* 2001).

by oxygen diffusing out from the YBCO layer. The process appears to be self-limited (this is not the case with a Pb counter-electrode, which "pumps out" oxygen so effectively that the underlying YBCO film can become insulating). Millimeter size contacts have typical resistances in the convenient range of 10 to 100Ω. These junctions do not yield characteristics as ideal as those that can be obtained by STM, apparently due to surface roughness and to the high sensitivity of the TDOS to faceting on the nanometer scale as demonstrated by the STM observations of Sharoni *et al.* (Sharoni *et al.*, 2001). (110) facets act actually as shorts. But the junctions have the significant advantage that they allow to take easily measurements as a function of temperature and applied magnetic field.

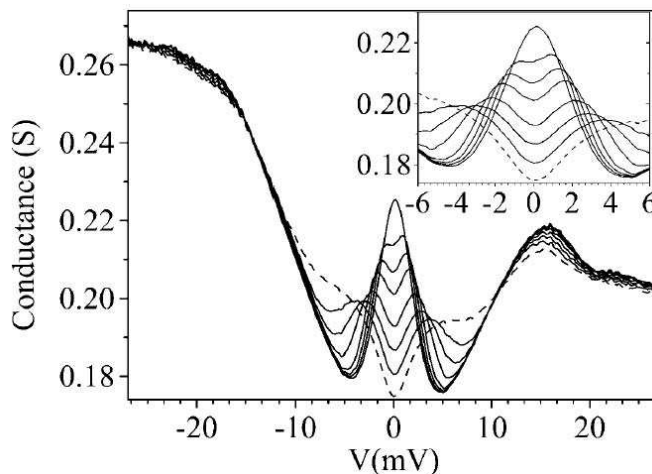


FIG. 16 Tunneling characteristics of an In/YBCO junction on a (110) oriented film at increasing magnetic fields of up to 6T. Insert: measurements in decreasing fields. (after Dagan and Deutscher 2001a).

A typical characteristic obtained by this method on a (110) oriented film is shown Fig.(16). Compared to STM data, the ZBCP is considerably smeared. On the other hand, a GLF is well pronounced. This GLF peak has been interpreted within the framework of the KT theory as resulting from surface roughness (Fogelstrom *et al.*, 1997), which has about the same effect as if the surface had an effective orientation intermediate between (100) and (110). Actually, there is not much difference between the characteristics of macroscopic junctions prepared on (100) and (110) oriented films. They show similar ZBCPs and GLFs. A quantitative fit to the data taking into account surface roughness has been presented by Fogelstrom *et al.* (Fogelstrom *et al.*, 1997). The GLF is well reproduced. Its peak position is somewhat below the value of the gap. Experimentally, its position is extremely reproducible from sample to sample (optimally doped), and from laboratory to laboratory. It is in fact one of the most reliable pieces of data to be found in the HTSC literature. Its position is 17 mV for optimally doped YBCO, with a variation of less than 1 mV between data originating from different laboratories. From Fogelstrom *et al.* (Fogelstrom *et al.*, 1997), the gap value might be up to 50% higher, or about 25 meV, depending on the exact surface orientation spread. Giving to the ASJ gap in optimally doped YBCO a range of 20 to 25 meV is a safe estimate.

3. High Z (110) contacts under magnetic fields

Lesueur *et al.* were the first to notice that a magnetic field can induce a split of the ZBCP in YBCO films, and proposed that it might be due to a Zeeman effect, under the assumption that the ZBCP itself is due to the presence of magnetic impurities in the vicinity of the barrier (Lesueur *et al.*, 1992). Covington *et al.* (Covington *et al.*, 1997) further studied this effect, which was given a different interpretation by Fogelstrom *et al.* (Fogelstrom *et al.*, 1997) in terms of a Doppler shift of the energy of the ASJ surface states. This Doppler shift is due to the superfluid velocity corresponding to the field induced Meissner currents. The experimental proof that the ZBCP is indeed not primarily due to the presence of magnetic impurities, was given by Krupke and Deutscher (Krupke and Deutscher, 1999) and by Aprili *et al.* (Aprili *et al.*, 1999). With films having a good in-plane orientation of the c -axis, they showed that the ZBCP field splitting is very anisotropic, being strong when the field is oriented perpendicular to the CuO_2 planes, and undetectable when it is in the orthogonal direction (Fig.17). It is in the first geometry that Meissner currents flow along the CuO_2 planes. If the ZBCP had been of magnetic origin, its splitting should have been isotropic.

In the model of Fogelstrom *et al.* (Fogelstrom *et al.*, 1997), the energy of the ASJ states is Doppler shifted by an energy equal to $v_S \cdot p_F \cos\Theta$, where v_S is the superfluid velocity associated with the Meissner currents, p_F is the Fermi momentum and Θ is the angle that the trajectory of a tunneling quasi-particle makes with the surface of the sample. At low fields, theory predicts that since v_S increases linearly with the applied field, so should the ZBCP splitting, as indeed observed experimentally (non linear effects may arise due to the presence of a s-wave channel, Fogelstrom *et al.* 2003). Saturation is predicted to occur at fields of the order of the thermodynamical critical field H_c , as observed by Covington *et al.*(Covington *et al.*, 1997) (Fig.18). The strong anisotropy of the ZBCP field splitting, and its field dependence, strongly support the idea that d-wave symmetry is at the origin of the ZBCP. The model of Fogelstrom *et al.* (Fogelstrom *et al.*, 1997) assumes that vortices do not penetrate in the sample up to fields of order H_c , or in other terms that there exists a strong Bean Livingston (Bean and Livingston, 1968) barrier. Since

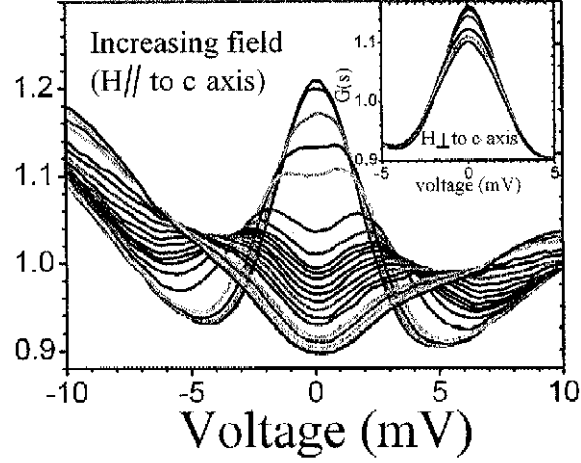


FIG. 17 Tunneling characteristics of an In/YBCO junction in increasing fields. The YBCO film has the (110) orientation and the field is oriented parallel to the surface of the film and parallel to the c-axis (itself in-plane oriented). Note (insert) that the splitting does not take place when the field is applied perpendicular to the c-axis. (After R. Beck privet communication)

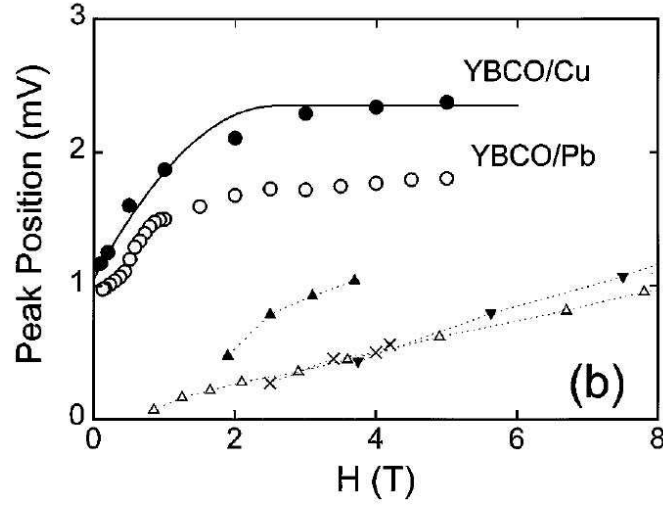


FIG. 18 Field dependence of the Zero Bias Conductance Peak for in-plane junctions to YBCO films. The fit for the YBCO/Cu contact is to the theory of Fogelstrom *et al.* (Fogelstrom *et al.*, 1997). (after Covington *et al.* 1997).

there is no such barrier against vortices exit in decreasing fields (Bussieres, 1976), a strong hysteresis of the ZBCP field splitting is expected. Again, this is in general agreement with experiment, the splitting being larger in increasing than in decreasing fields (Krupke and Deutscher, 1999). In fact, according to the Doppler shift model based on the Bean Livingston currents, there should be no ZBCP splitting at all, or only a small one, in decreasing fields. It is also expected that the splitting should be strongly decreased at thickness smaller than the London penetration depth λ , for which Meissner currents reduce as the thickness divided by λ . Both predictions are again in agreement with early results obtained on films that had the (100) orientation (Krupke and Deutscher, 1999) or the (103) orientation (Covington *et al.*, 1997). For such films, the very existence of the ZBCP is supposedly due to surface roughness. Later results, obtained on films that did have the (110) orientation, show a more complex behavior. In particular there is a strong splitting in decreasing fields, and it persists even at small thickness (Beck *et al.*, 2003; Dagan and Deutscher, 2001b). This behavior raises questions that will be discussed in the last section of this review.

V. ASJ SPECTROSCOPY AND THE PSEUDO-GAP ISSUE

ASJ spectroscopy allows a good determination of the gap in the cuprates, it gives solid evidence that they have well defined quasi-particles and provides a good estimate of their mass renormalization. ASJ spectroscopy is also a phase sensitive tool. More will be said on this last topic when we discuss the occurrence of minority components of the order parameter in the last section of this review. It turns out that ASJ spectroscopy also sheds light on the possible origins of the pseudogap, one of the least understood features of the cuprates.

A. Manifestations and possible origins of the pseudogap

There exists converging experimental evidence from NMR spin susceptibility measurements (Alloul *et al.*, 1989), heat capacity measurements (Tallon and Loram, 2001), ARPES (Ding *et al.*, 1996), optical measurements (see the review by Timusk and Statt, Timusk and Statt 1999) and from tunneling experiments (Miyakawa *et al.*, 1997; Racah and G.Deutscher, 1996; Renner *et al.*, 1997) that in underdoped cuprates there is a loss of states at the Fermi level below a temperature $T^*(p)$ that increases as the doping p is decreased. T^* and T_c have opposite variations as p is reduced below the optimum level p_M . This loss of states occurs over a certain energy range, called the pseudogap, which can be measured by different spectroscopic methods. There are until to day vastly conflicting views on its origin. From a phenomenological stand point, these views belong to one of two possible classes: either the pseudogap is a high temperature precursor of the superconducting state, or it is strictly a normal state property, with no direct relation to superconductivity. In the first case, T^* is the temperature below which a pairing amplitude appears, without the phase coherence which is achieved at the lower temperature T_c ; it follows necessarily that $T^* > T_c$. In the second case, T^* being a normal state property is not necessarily larger than T_c . In the first case, there cannot be a crossing point between $T^*(p)$ and $T_c(p)$; in the second case, there may be one.

Friedel (Friedel, 1988, 1989) has applied the concept, developed by Mott to describe the effects of coherent diffraction of valence electrons from a local atomic order in liquid or amorphous metals or Hume Rothery alloys, to the case of local 2D anti-ferromagnetic (AF) order. The term pseudogap that he introduced describes a DOS resembling that resulting from long range AF order, with a gap and peaks at the gap edges, but with states within the gap and broadened peaks.

By contrast, other authors have given to the pseudogap the meaning of a high temperature precursor to superconductivity. Chen *et al.* (Chen *et al.*, 2004) have investigated the regime of BCS to BE crossover with the emphasis on finite temperature effects. They find that in the crossover region, the order parameter is distinct from the gap in the single particle excitation spectrum, going to zero at T_c while the gap remains finite, and goes smoothly into the pseudogap regime above T_c . In the ground state, as seen in a low temperature spectroscopic experiment, there is only one single energy scale, the order parameter and the gap being identical. In yet a different approach, Bernevig *et al.* (Bernevig *et al.*, 2003) have studied the effect of strong Coulomb effects on superconductivity. They find that these effects generate a d-wave gap, and at the same time reduce the superfluid density. The stronger they are, the larger the gap value and the smaller T_c will be because of Kosterlitz-Thouless effects (Emery and Kivelson, 1995). The transition to the insulating AF state occurs at half filling. If Coulomb effects reduce (as may be expected in the overdoped region), there is a smooth transition to a BCS superconductor. In this model as well as in the BCS-BE crossover scheme, the pseudogap is a manifestation of incipient superconductivity.

In a different approach, Perali *et al.* (Perali *et al.*, 2000) have studied the consequences of a strong anisotropy, both the effective interaction and the Fermi velocity being momentum dependent. At the anti-nodes the interaction is strong and the Fermi velocity small, and vice versa at the nodes. One possible mechanism of a strong momentum dependence is a charge instability for stripe formation, occurring below a line $T^*(p)$ that starts from a Quantum Critical Point (QCP) at $T = 0$ near optimum doping. Other theories have emphasized the role of fluctuations around a Quantum Critical Point (QCP), one of its manifestations being an imaginary component of the order parameter appearing on one side of the QCP (Ng and Varma, 2004; Sachdev, 2000).

Renner *et al.* (Renner *et al.*, 1997) performed STM measurements on BSCCO single crystals at different doping levels, and observed a pseudogap (with a substantial density of states within it) above T_c , merging into the gap in the superconducting state below T_c . In underdoped crystals, a pseudogap could be observed up to room temperature (Fig.19). Even in overdoped samples, a pseudogap was seen to persist a few 10K above T_c . In other terms, $T^*(p)$ and $T_c(p)$ as measured by tunneling in BSCCO do not cross each other. This behavior is compatible with the pseudogap possibly being a precursor of the superconducting gap, as proposed by the authors. An increase of the gap was also measured by break junctions on underdoped BSCCO by Miyakawa *et al.* (Miyakawa *et al.*, 1997).

On the other hand, Tallon *et al.* (Tallon and Loram, 2001) have concluded from an analysis of heat capacity data on a number of cuprates that $T^*(p)$ and $T_c(p)$ do cross each other, $T^*(p)$ following a linear behavior that extrapolates at zero temperature to a universal "critical" concentration $p_c = 0.18$ holes/Cu. They conclude that T^* is not directly

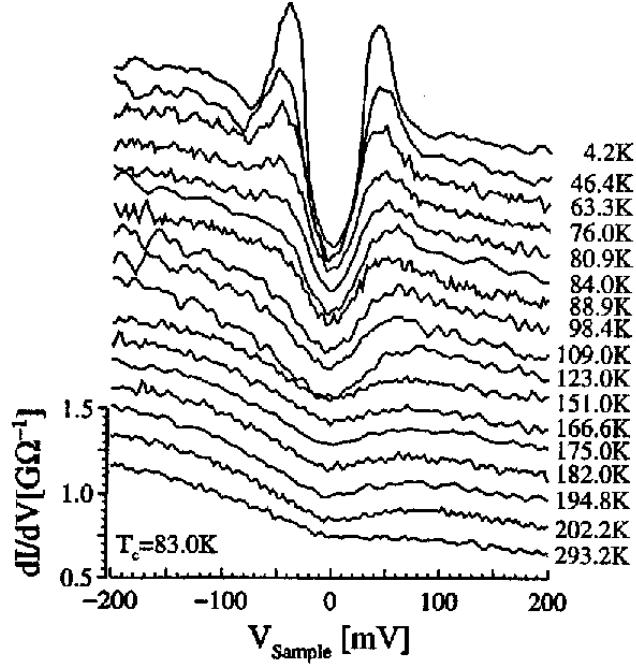


FIG. 19 STM characteristics measured on an underdoped $Bi_2Sr_2CaCu_2O_8$ single crystal, at temperatures ranging from 4.2K up to room temperature. A conductance dip persists up to the highest temperature. Note however the change in the dip amplitude when going from 123K to 151K. (after Renner *et al.* 1997).

related to superconductivity.

Very recently, Alff *et al.* (Alff *et al.*, 2003) have reported that in the electron doped compounds PrCeCuO and LaCeCuO, a pseudogap develops only at low temperatures $T < T^* < T_c$, as can be seen by applying magnetic fields strong enough to destroy superconductivity, and conclude that the pseudogap cannot be a precursor to the superconducting state. The absence of a pseudogap opening above T_c in the electron doped cuprates was also noted by Kleefisch *et al.* (Kleefisch *et al.*, 2001), and its presence below T_c noted by Qazilbash *et al.* (Qazilbash *et al.*, 2003).

These results (and many others that we have not quoted) do not allow one to draw a general conclusion regarding the origin of the pseudogap. It may be that different kinds of measurements, such as tunneling and heat capacity, "see" different pseudogaps. Additionally, it could also be that the pseudogap has different origins in different cuprates. For a recent review on the pseudogap, see Timusk and Statt (Timusk and Statt, 1999).

B. ASJ spectroscopy in the pseudogap regime

The first important observation is that strong ASJ reflections are observed in the pseudogap regime. This is particularly true for ASJ bound states. ZBCPs have been observed in strongly underdoped YBCO (Dagan *et al.*, 2000) and BSCCO (Sinha and Ng, 1998). They persist up to T_c where they vanish. The second observation is that in the pseudogap regime gap values determined by ASJ spectroscopy and single particle spectroscopies (tunneling or ARPES) are different, while they roughly agree in the overdoped regime (Deutscher, 1999).

In underdoped YBCO, Yagil *et al.* (Yagil *et al.*, 1995) have reported measurements of ASJ reflections by point contact on a-axis films [(100) oriented surface] yielding a gap value of 13 meV. The enhancement of the conductance below the gap is weaker than in optimally doped YBCO. Giaever tunneling on similarly underdoped a-axis films, with T_c values in the range of 40 to 60K, gives a gap of 40 to 50 meV (Racah and G.Deutscher, 1996). (Fig.20)

As mentioned above, in an underdoped BSCCO junction close to the (110) orientation and having a $T_c = 70K$, Sinha and Ng (Sinha and Ng, 1998) obtained from their fit to the data an ASJ gap of 13 meV. This is much smaller than the 50 meV STM gap value at similar doping (Renner *et al.*, 1997). Aubin *et al.* (Aubin *et al.*, 2002) prepared tunnel junctions on optimally doped single crystal BSCCO having a surface passivated by a thin CaF_2 layer. Crystals were cut and polished so as to expose (100) and (110) oriented surfaces. On (100) surfaces, broad Giaever-like tunneling curves were obtained with maxima at 37 meV, which is in agreement with STM data (Renner *et al.*, 1997). On (110)

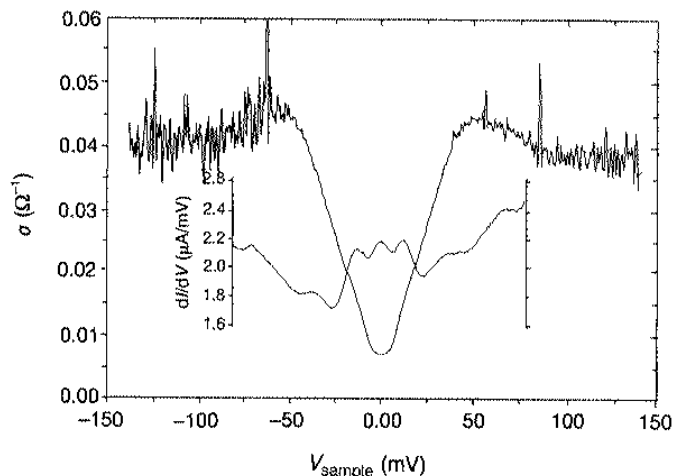


FIG. 20 Comparison between an ASJ (inside graph) and a Giaever characteristic measured on similarly underdoped YBCO samples. Note the difference in energy scales: about 15 meV for the ASJ reflection edge, and 50 meV for the Giaever gap. (after Deutscher 1999).

surfaces the conductance characteristic has the shape typical of high Z junctions for that orientation, with a high ZBCP followed by a dip before recovery to the normal state conductance. Recovery occurs in the range of 20 to 30 meV (fig. 4a and fig.2 of Aubin *et al.* 2003), which we would expect corresponds to the range of possible gap values. A fit to this (110) data, considered as reasonable by the authors, was nevertheless given with a gap value of 37 meV. D’Gorno and Kohen (D’Gorno and Kohen, 1998) obtained point-contact junctions on a nearly optimally doped (may be slightly overdoped) BSCCO single crystal, that could be fitted very well to a (100) orientation with a gap value of 20 meV and $Z = 0.8$ (Fig.9). We would conclude that, for BSCCO, ASJ spectroscopy (low Z (100) contacts, moderate and high Z (110) contacts, both sets of data being dominated by ASJ reflections) gives for BSCCO a gap of 20 to 30 meV at or near optimum doping, and less than 15 meV in underdoped samples. By contrast, Giaever tunneling gives gap values of 30 to 40 meV at optimum doping and 40 to 50 meV in underdoped samples. Recently, a detailed STM study on BSCCO cleaved crystals, systematically scanning large areas of the crystal, have shown that up to energies in the range of 20 meV, the single particle tunneling spectra are quite homogeneous across the sample’s surface even in underdoped samples (McElroy *et al.*, 2004). By contrast, gap values as determined by the bias at which the conductance is at a maximum, are quite inhomogeneous and range from 20 meV up to 70 meV. Spectra showing the larger gaps have weak coherence peaks. They correspond to anti-nodal states, which are quite inhomogeneous in space. These observations are consistent with our report of strong ASJ reflections ranging in energies up to about 20 meV (Deutscher, 1999). This appears to be the energy scale of the superconducting condensate. It does not increase in the underdoped regime.

On LSCO, Gonnelli *et al.* (Daghero *et al.*, 2002) have reported measurements of ASJ gaps that decrease in the underdoped regime, as also seen by Dagan *et al.* (Dagan and Deutscher, 2001a). Like in YBCO and BSCCO, Giaever gaps do increase in underdoped samples.

The following experimental picture then emerges. Strong ASJ reflections occur in optimally doped and overdoped samples for all surface orientations. In underdoped samples, ASJ reflections are weakened on (100) surfaces, but remain strong on (110) surfaces. Gap values obtained from conductance characteristics dominated by ASJ reflections are equal to or smaller than gap values obtained from single particle tunneling. They decrease in the underdoped regime, following at least qualitatively the doping dependence of T_c (Fig.21).

At low temperatures, there exists in most cuprates a tunneling pseudogap that increases as doping is reduced. The pseudogap appears in the normal state below a temperature T^* , which can be higher or lower than T_c . In some cuprates, such as BSCCO, $T^* > T_c$ in most (if not all) the doping range. In other cuprates, the curves $T^*(p)$ and $T_c(p)$ cut each other at some doping level p^* . This is the case of YBCO and even more clearly of the electron-doped compounds. For $p < p^*$, the pseudogap appears above T_c and is larger than the ASJ gap. For $p > p^*$, the ASJ gap and the Giaever gap converge. In that regime the pseudogap does not appear above T_c , but in electron doped cuprates it may be seen below T_c by applying a field strong enough to quench superconductivity.

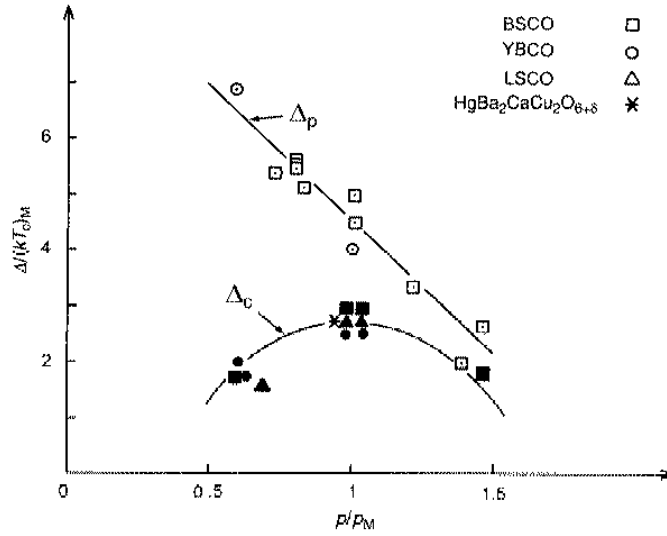


FIG. 21 Behavior of ASJ and Giaever (or ARPES) energy scales as a function of doping in different cuprates. The ASJ scale (Δ_c) follows the same behavior as T_c does, while the Giaever scale (Δ_p) keeps raising as the doping is reduced (after Deutscher 1999).

C. Compatibility of ASJ reflections and pseudogap models

1. RVB and other models emphasizing strong correlation effects.

A pseudogap is already implicit in the Resonating Valence Bond (RVB) model of Anderson (Anderson, 1987), which postulates that electron correlations are the key ingredient in the superconductivity of the cuprates. There may be however one major difficulty with this model regarding ASJ reflections, which concerns the nature of electronic excitations. In the RVB model, these are not the usual quasi-particle excitations we are familiar with in metals, but rather excitations that do not carry at the same time charge and spin (holons and spinons). There is no electron-hole symmetry, and it is not clear whether under these circumstances one could at all have strong ASJ reflections, whose very existence imply electron-hole mixing : in a Saint James cycle, an excitation is electron-like half of the time, and hole-like the other half.

This difficulty may be overcome in other models where strong electron correlations play also a key role. They include fermion-boson models with electron pockets developing near the nodes as doping is increased (Altman and Auerbach 2002; for earlier fermion-boson models, see Friedberg and Lee 1989; Ranninger *et al.* 1995). In the condensed state, there is a bosonic field that generates a superconducting gap *a la* BCS in the electron pockets, and excitations from this gap would have the usual electron-hole symmetry.

In another recent model originally proposed by Laughlin (Bernegiv *et al.*, 2003; Laughlin, 2002), strong electron correlations come on top of a conventional BCS Hamiltonian. In contrast with the RVB model, the nature of electronic excitations is then identical to that in ordinary metals, there are thus no problems with ASJ reflections. Strong correlations increase continuously the value of the BCS gap, while at the same time the superfluid density is reduced, eventually leading to the destruction of superconductivity as a macroscopic coherent phenomenon (Emery and Kivelson, 1995). The (pseudo) gap appearing at high temperatures is then a precursor of superconductivity, before it is quenched altogether. As we shall see below, there are problems with this part of the model.

2. The semiconductor-superconductor and strong coupling models

Pistoiesi and Nozieres (Pistoiesi and Nozieres, 2000) have calculated the conductance of N/S contacts within two models compatible with the existence of a gap in the DOS above T_c : one where it is a normal state property, namely there is a semiconducting gap Δ_o due to a competing order such as a Charge Density Wave (CDW), which has no direct relation to superconductivity (Nozieres and Pistoiesi, 1999); and another one, in which the pseudogap is a manifestation of a crossover to strong coupling (Bose Einstein limit) where the energy necessary to break a pair can be much larger than $k_B T_c$ (Leggett, 1980; Nozieres and Schmitt-Rink, 1985).

In the normal state pseudogap scenario, ASJ reflections are reduced by the competing order that prevents the

full conversion of incoming quasi-particles into superfluid. In the strong coupling limit, ASJ reflections are reduced because of a mismatch of the Fermi wave vectors when the gap approaches the Fermi level. In both cases, there exists an energy gap E_g which is a combination of the normal state gap, or energy necessary to break a preformed pair, and of the superconducting order parameter. In both models, the BTK reflection coefficient $A(\varepsilon)$ is reduced below E_g , this reduction becoming substantial if E_g is large compared to the order parameter Δ . No strong ASJ reflections can then occur.

In the specific example of the semiconductor-superconductor model, the CDW order (Δ_0) induces Bragg reflections and the superconducting order (Δ_m) ASJ reflections. The strongest order determines the penetration depth of the evanescent wave. If Δ_0 is larger, the specular Bragg reflection will build up before the ASJ reflection does. The later will therefore be weak. A similar conclusion is reached in the strong coupling limit. In the calculated conductance characteristic, there is no structure at the bias equal to the superconducting order parameter if $\Delta_0 > \Delta_m$, or in the strong coupling limit.

These results are of a generic nature. They apply to different models of the pseudogap such as the BCS to BE crossover (Chen *et al.* 2004 or models emphasizing strong correlations Bernegiv *et al.* 2003, or models of competing orders Castellani *et al.* 1997). They are not in agreement with the experimental findings of strong ASJ reflections, and of an ASJ energy scale smaller than the Giaever gap, in the pseudogap regime, *if one assumes that the competing order parameter (or the strong coupling effects) dominates all around the Fermi surface over the superconducting order parameter.*

Note however that the calculation assumes that the normal state gap is a full gap, namely that in the normal state there are no states below it. This is of course an oversimplification of the experimental situation. For PCCO, in which the normal state TDOS has been measured at low temperatures (Alff *et al.*, 2003), the zero-bias conductance is still about 80% or more of its normal state value, so there are in fact many states below the pseudogap. Such a high DOS in the pseudogap region is obtained in the model of Friedel and Kohmoto (Friedel and Kohmoto, 2002). If these states are conducting, one might expect structures in the conductance characteristic at both biases: the superconducting order parameter and the pseudogap scales. Two energy scales: one where the conductance goes down, marking the ASJ gap, and one where it goes up, marking the pseudogap, are indeed visible in the data of Yagil *et al.* (Yagil *et al.*, 1995). But no conductance calculations are available for the Friedel-Kohmoto (Friedel and Kohmoto, 2002) pseudogap model that we could compare quantitatively to experiments.

An alternative approach has been tried by Pistoiesi (Pistoiesi, 1998), who has shown that a critical current effect may in fact introduce in the conductance characteristic a structure at a bias value which is typically the phase stiffness Λ , which limits T_c in the strong coupling or weak superfluid density limit. As shown for instance by Emery and Kivelson (Emery and Kivelson, 1995), when the superfluid density is very small, T_c is determined by:

$$kT_c = (16\pi^3)^{-1}(\Phi_0)^2(a/\lambda^2) \quad (5.1)$$

where Φ_0 is the flux quantum, λ the in-plane London penetration depth and a a length scale equal to the coherence length in the direction perpendicular to the CuO planes or to the inter-plane distance, whichever is larger. Pistoiesi finds that a critical current effect will reduce the conductance at a voltage V_c given by:

$$eV_c = \Lambda(k_F \xi_{phase})^{-1} \quad (5.2)$$

where $x_{i_{phase}}$ phase has been calculated by Pistoiesi and Strinati (Pistoiesi and Strinati, 1996) and by Marini *et al.* (Marini *et al.*, 1998). In the vicinity of the BCS to BE crossover, $k_F x_{i_{phase}} \approx 1$, and $eV_c \approx \Lambda \approx kT_c$, in agreement with experimental results (Deutscher, 1999).

3. Two gap model

The Rome group (Perali *et al.*, 2000) has extended the semiconductor-superconductor model of Pistoiesi and Nozieres (Pistoiesi and Nozieres, 2000) to the case of a d-wave order parameter. In this model, the competing order parameter dominates over the superconducting one *only in the anti-node regions*. Specifically the origin of the pseudogap lies in the vicinity of a Charge Density Wave (CDW) (Benfatto *et al.*, 2000) line $T^*(p)$, as mentioned above, but from a phenomenological standpoint their main results are given in terms of a gap $\Delta(\phi)$ which is dominated by the pseudogap Δ_p near the anti-nodal points and by the superconducting order parameter near the nodes. They argue in favor of the weak coupling limit $\Delta < t$, where t is the nearest neighbor interaction term in the tight binding approximation, so that T_c is equal within a numerical factor to the energy scale that governs the behavior of Δ near the nodes. In the over-doped regime, $\Delta(\phi)$ follows the d-wave law $\Delta(\phi) = \Delta(0)\cos 2\phi$ over the entire angular range. In the underdoped regime, the value of the gap at the nodal points is uncorrelated to the (larger) characteristic energy scale near the nodes.

This model is qualitatively in agreement with the results of ASJ spectroscopy on (110) surfaces in the under-doped regime as described above. The pseudogap near the anti-nodal points is larger than the value that the superconducting order parameter would have in the absence of this pseudogap (in the language of Nozieres and Pistoiesi, $\Delta_o > \Delta_m$ near the anti-nodal points). Thus, these regions do not contribute to the ASJ reflection amplitude because for the corresponding \mathbf{k} vectors normal quasiparticle reflection occurs before conversion to the condensate takes place. Hence, the only energy scale that will appear in ASJ spectroscopy will be that which characterizes the angular dependence of the gap near the nodes, which is the superconducting order parameter, itself proportional to T_c . The fact that for all cuprates studied so far the ASJ spectroscopy energy scale varies with doping as T_c does, just means that these cuprates are basically in the weak coupling limit as assumed by the Rome group.

More generally, a momentum dependence of the interactions leading to the pseudogap, whatever its origin may be, seems to be a necessity if agreement with ASJ experiments is to be achieved. This is because these experiments tell us that there is no pseudogap around the nodes. Theories that do not include a momentum dependence, such as those of Chen *et al.* (Chen *et al.*, 2004), or Bernevig *et al.* (Bernevig *et al.*, 2003) for which the pseudogap is a d-wave gap that becomes the superconducting gap at low temperatures, do not seem to be compatible with the observation of strong ASJ reflections in the underdoped regime.

4. Some comments on the pseudogap

In a previous publication (Deutscher, 1999) I left open the question of the origin of the pseudogap: whether the loss of states at the Fermi level that starts below T^* is due to an emerging pairing amplitude (a strong coupling effect), or whether it bears no direct relation to superconductivity. Theoretical progress in the analysis of experimental results known at this time and new experiments reviewed in this section, and particularly conclusions drawn from the observation of strong ASJ reflections in the pseudogap regime, present in fact serious difficulties for both kinds of models, at least if no momentum dependence is included. Yet, I believe that the balance now tilts somewhat against the preformed pairs scenario.

The formation of true bound pairs above T_c , in the sense of a negative chemical potential with respect to the bottom of the conduction band, requires a binding energy of the order of a fraction of the band width, say of the order of the eV. Pseudo-gap values determined by ARPES and tunneling do reach at most 10% of this value. So there cannot really be bound pairs. More specifically, for $(\Delta/EF) \approx 0.1$ as seen experimentally, strong coupling theory (Pistoiesi and Strinati, 1996) tells us that the two length scales ξ_{pair} (the size of a pair) and ξ_{phase} (the size of a vortex core) differ only by a few %, and so should the corresponding energy scales. Instead, for moderately underdoped samples (T_c about half of its maximum value), the pseudogap and the ASJ gap differ by a factor of about 4. According to this analysis, the pseudogap is not a strong coupling effect. Additionally, there should be at low temperatures only one energy scale in the superconducting state (Chen *et al.*, 2004). In the under-doped regime, this is not the case since the Giaever and the ASJ gaps have opposite doping dependences (Fig.21). The recent experiments of McElroy *et al.* (McElroy *et al.*, 2004) also establish that there is no correlation between homogeneous, low energy excitations in the nodal regions, and large gaps in the anti-node regions.

Ruling out the pseudogap as a *homogeneous* precursor of superconductivity *in real space and in momentum space* does not mean that the cuprates are strictly in the BCS weak coupling limit. In fact, they are not far from the BCS to BE crossover, defined as shown by Pistoiesi and Strinati by the condition $(k_F \xi_{pair}) = 1$. One of the manifestations of this proximity is the Uemura plot $T_c \propto \lambda^{-2}$ followed by all underdoped cuprates (Uemura, 2002). Another one is the observation of strong fluctuation effects in the heat capacity transition. These measurements allow us in fact to draw a fine distinction between different cuprates in terms of their proximity to the BCS-BE crossover. The heat capacity transition in YBCO can be analyzed in terms of a mean field jump with additional fluctuation effects (Junod *et al.*, 1999; Marcenat *et al.*, 1996). These fluctuation effects become quite weak in overdoped samples (Junod *et al.*, 1999), for which the transition becomes more and more BCS like as doping is increased. A contrario, no mean field jump can be identified in BSCCO, for which fluctuation effects clearly extend several 10K above T_c , consistent with it being closer to the BCS-BE crossover than is YBCO. Enhanced fluctuations may also reflect the more 2D nature of BSCCO. But a closer proximity of BSCCO to the BCS-BE crossover is also consistent with spectroscopy results. At optimum doping, the Giaever gap in BSCCO (about 30 to 40 meV) is larger than that in YBCO (about 20 meV). Also, the coherence length as measured by the radius of the vortex core, is shorter in BSCCO than it is in YBCO (Fischer *et al.*, 1998). These are clear indications that at comparable doping levels BSCCO is closer than is YBCO to the condition $(k_F \xi_{pair}) = 1$.

The STM pseudogap data of Renner *et al.* (Renner *et al.*, 1997)(Fig.19) on underdoped BSCCO reveals that there may be a difference between characteristics measured up to 121K, and above that temperature. The former bare indeed a strong resemblance with those measured immediatly below T_c , while the later show only a weak anomaly that remains essentially temperature independent up to room temperature. This suggests that there might

be both a superconductivity related pseudogap between T_c and 120 to 130K, and a normal state pseudogap at higher temperatures. More data is needed here to clarify the situation.

As for YBCO, the quasi-mean field behavior of the heat capacity at optimum doping is fully consistent with the absence of a pseudogap in tunneling, and with the fact that the Giaever and ASJ gaps are identical. YBCO is in fact the only cuprate that clearly breaks away from the Uemura plot. By overdoping it with oxygen up to O_7 , its superfluid density can be increased up to a factor of two compared to its value at optimum doping, while T_c remains almost constant (it only goes down by a few degrees). (Bernhardt *et al.*, 1995) In the overdoped regime, YBCO presents all the characteristics of a strict BCS superconductor: a critical temperature independent from the superfluid density, a sharp heat capacity transition, identity between the Giaever and ASJ gaps. It would be really surprising if nearly optimum doped BSCCO, not so different after all, would show precursor effects of superconductivity up to room temperature. May be such strong precursors effects could be found in more strongly underdoped cuprates, if the condition ($k_F \xi_{pair}$) could be reached. Research is still going on in this area.

VI. SYMMETRY STUDIES AND SPIN EFFECTS

In this last section, I would like to mention two topics of current interest in ASJ spectroscopy: effects on the symmetry of the order parameter in the cuprates of different perturbations such as non-optimum doping, applied magnetic fields and proximity with a normal metal. A few words on spin effects are added at the end of this section.

Phase sensitive experiments are the only ones that can lead to definite conclusions regarding the symmetry of the order parameter. Such were the corner SQUID experiments of Wollman *et al.*, (Wollman *et al.*, 1993) and those of Tsuei and Kirtley (Tsuei and Kirtley, 2000a,b) that have established that the order parameter in the cuprates has a dominant d-wave symmetry. These experiments have however left two interesting questions unanswered. First, because they measure phase differences of the order parameter at surfaces or interfaces (grain boundaries), they are not sensitive to possible changes of the symmetry between the surface and the bulk. Muller has recently raised this issue, and has argued that a s-wave channel may in fact dominate in the bulk (Muller, 2004). Second, they are not well suited to detect the existence of a small imaginary minority component. In the experiments of Tsuei *et al.* for instance, the signature of pure d-wave symmetry is a spontaneous half flux quantum at a tri-crystal junction. A small id_{xy} component would only slightly modify this flux value, and will be undetected if this change is smaller than the margin of error in the measured value. Additionally, these experiments were evidently not designed to study possible effects of strong applied fields on the symmetry of the order parameter. ASJ spectroscopy is ideally suited to answer such questions. ASJ bound states are very sensitive to the existence of a small imaginary component of the order parameter, which has the immediate effect of removing the nodes. And ASJ spectroscopy can be easily performed under applied fields.

The formalism of Kashiwaya and Tanaka (Kashiwaya *et al.*, 1995) can be used to calculate I(V) characteristics for any order parameter $\Delta(\phi)$. For instance for:

$$\Delta(\phi) = \Delta_0 \cos 2\phi + i\Delta_1 \sin 2\phi \quad (6.1)$$

(the $d + id$ symmetry), the (110) ZBCP is split (peak to peak) by Δ_1 . The same holds for a $(d + is)$ symmetry. Such symmetries have been discussed by Yang and Hu (Hu, 1994). These order parameters break time reversal symmetry, implying the flow of boundary currents (Laughlin, 1998).

A. ASJ bound states under applied fields

The effect of Meissner screening currents also leads to a split of the ZBCP as discussed in section IV. When a ZBCP splits under an applied field, how can we know whether it does so because of field induced Meissner currents, or because it is the field itself (not the currents) that has induced a change in the symmetry of the order parameter, as proposed for instance by Laughlin (Laughlin, 1998)?

Beck *et al.* (Beck *et al.*, 2004) have remarked that the current effect should cancel out in *decreasing fields*, because it is known that there is no Bean-Livingston surface barrier against flux *exit*. A ZBCP split in decreasing fields, if observed, should therefore be primarily a field effect, and not a current effect. They have measured such a split in the characteristics of junctions prepared on (110) oriented YBCO films, and have shown that it follows the law:

$$\delta(B) = AB^{1/2} \quad (6.2)$$

where 2δ is the ZBCP split expressed in meV, $A = 1.1 \text{ meV}/T^{1/2}$ and B is the field in Tesla. This law was seen to hold up to a field of 16T (Fig.22). It is in agreement with a prediction by Laughlin (Laughlin, 1998) regarding the amplitude Δ_1 of a field induced id_{xy} component. Node removal costs an energy proportional to $|\Delta_1|^3$, but an energy proportional to $(B \cdot \Delta_1)$ is gained because of the magnetic interaction with the field of the moment produced by the *circulating* currents proportional to the amplitude of the id_{xy} component. Minimization of the sum of the two terms leads to a law of the form 6.2. The value of the coefficient A found experimentally is in quantitative agreement with theory.

B. Doping effect on the symmetry

Covington *et al.* (Covington *et al.*, 1997) have reported a spontaneous split of the ZBCP in YBCO in-plane tunneling, and have interpreted it as an effect of spontaneous time reversal symmetry breaking. Fogelstrom *et al.* (Fogelstrom *et al.*, 1997) have proposed that this spontaneous split results from the emergence at the surface of an *is* component of the order parameter, an emergence made possible by the local depression of the main d component.

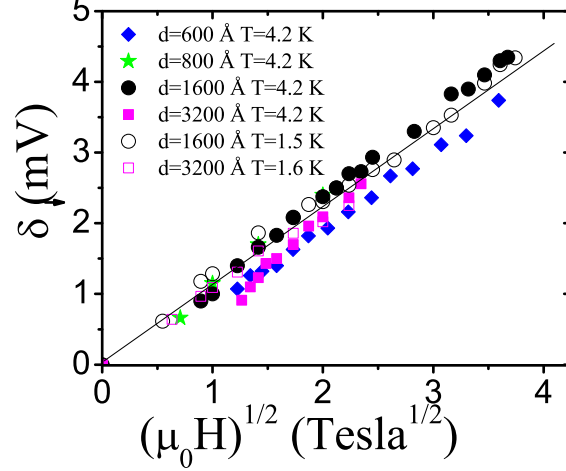


FIG. 22 Split of the ZBCP in a number of In/YBCO junctions on (110) oriented films, of different thickness, measured in decreasing fields. The split follows a square root law, with a coefficient of the order of $1 \text{ mV}/T^{1/2}$. (after Beck *et al.* 2004)

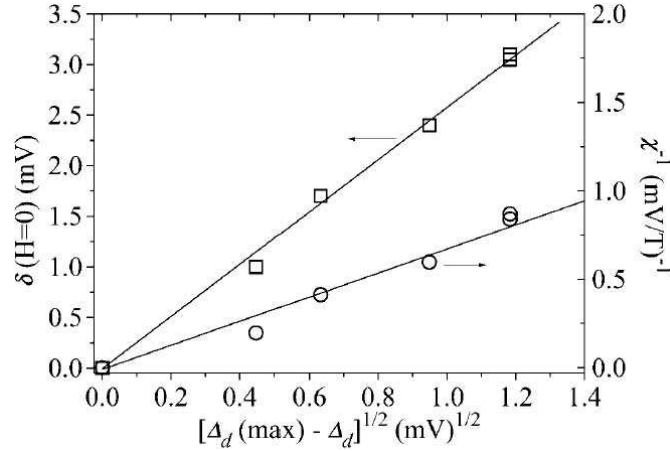


FIG. 23 Dependence of the spontaneous ZBCP split in In/YBCO junctions on (110) oriented films, as a function of a parameter proportional to the doping level. Overdoping was achieved by increasing the oxygen content. A spontaneous split is only found in overdoped samples. The inverse of the initial slope of the ZBCP field splitting, or susceptibility, is also shown. The susceptibility diverges near optimum doping. The behavior of the spontaneous splitting and of the susceptibility are indicative of the presence of a quantum critical point near optimum doping, beyond which the order parameter develops a small imaginary component (after Dagan and Deutscher 2001a).

Dagan *et al.* (Dagan and Deutscher, 2001a) have reported that in YBCO the spontaneous ZBCP split occurs only in overdoped samples, where it follows the law:

$$\delta = C(p - p_M) \quad (6.3)$$

where p is the doping level and p_M its optimum value (at maximum T_c) (Fig.23). These results were obtained on oxygen overdoped films. A similar law was reported by Sharoni *et al.* (Sharoni *et al.*, 2002) on Ca overdoped YBCO films.

There is no direct way to know from tunneling measurements whether the spontaneous imaginary component supposedly responsible for the ZBCP split has the s or the d_{xy} symmetry. An s symmetry would mean that the strength of the sub-dominant s -channel, emerging at the surface as postulated by Fogelstrom *et al.*, (Fogelstrom *et al.*, 2003), has a strong doping dependence. Alternatively, the imaginary component might be a bulk property. Friedel and Kohmoto (Friedel and Kohmoto, 2002) have predicted that an id_{xy} component should appear in the overdoped

regime, while the symmetry is pure d-wave in the underdoped one, as reported by Dagan *et al.* (Dagan and Deutscher, 2001a). In their theory, the d-wave symmetry does not come about because of the interaction responsible for pairing, but rather due to the symmetry of the carriers wave function. Yet another possibility is that the change of symmetry at optimum doping reflects the existence of a quantum critical point (Dagan and Deutscher, 2001a; Sachdev, 2000).

Some ASJ data indicating a possible change of symmetry near optimum doping are also available on LSCO (Achsaf *et al.*, 1996; Dagan *et al.*, 2000) and on the electron doped PCCO (Qazilbash *et al.*, 2003). The electron doped cuprates had long been considered an exception to the d-wave symmetry (Fournier *et al.*, 1998), inter alia because of the absence of a ZBCP (Alff *et al.*, 1997). However, more recent tri-crystal experiments (Tsuei and Kirtley, 2000a,b), indicated a d-wave symmetry. But very recently, a change of behavior of PCCO has been reported as a function of doping, including the ASJ data of Qazilbash (Qazilbash *et al.*, 2003) already mentioned and penetration depth data in overdoped PCCO is better fitted by a nodeless order parameter (Skinta *et al.*, 2002). It could well be that the long standing controversy on the symmetry of the order parameter in the electron doped cuprates is on its way towards a resolution in terms of a doping dependence. Electron doped cuprates are naturally overdoped, which may explain the early results pointing to a nodeless behavior.

A doping dependent symmetry, if confirmed as a bulk property, would be of some consequence for our understanding of the HTS mechanism. Many of the proposed theoretical models, such as (t,J) models, give a prominent role to the anti-ferromagnetic coupling parameter J , with this interaction being the primary coupling channel. A pure d-wave symmetry follows necessarily in such models, at any doping level. On the contrary, in the model of Friedel and Kohmoto, the d-wave symmetry does not follow from the pairing interaction itself, but rather from the symmetry of the electronic wave functions, as they are affected by the proximity of the AF state. In that case, Friedel and Kohmoto show that the order parameter symmetry changes with doping, and in a manner that fits the experimental observations of Dagan *et al.* (Dagan and Deutscher, 2001a), an imaginary component appearing beyond optimum doping. In fact, it has been claimed very recently on the basis of high temperature expansions in the thermodynamical limit that the one band (t, J) model does not lead to a superconducting state (Pryadko *et al.*, 2004), contrary to what had been proposed earlier from numerical work on finite size systems. So it may be that more conventional interactions such as the electron-phonon interaction will now receive renewed attention.

C. Proximity effect on the symmetry

Wei *et al.* (Wei *et al.*, 1998) noted the possibility of a proximity effect between a normal tip and YBCO resulting in a partial s-wave character of the order parameter in the later. Gonnelli *et al.* (Daghero *et al.*, 2002) studied low Z contacts ($Z < 0.5$) on LSCO samples as a function of Sr doping. They analyzed the conductance characteristics in terms of a complex order parameter and determined the intensity of each component as a function of doping. They found them to be of the same order. This is in sharp contrast with results obtained on high Z contacts with YBCO, described in the above sub-section. There, the *is* (or *id*) component is never more than a fraction of the dominant d component. Kohen *et al.* (Kohen *et al.*, 2003) have recently reported a systematic study of the intensity of the minority component in YBCO as a function of the barrier transparency, for contacts point contact having all $Z < 1$ (fig.24). They conclude that the value of Z has a strong influence on the intensity of this component, which according to their analysis has the *is* symmetry. At low Z values, both components have similar values. The *is* component diminishes quickly for $Z > 0.5$. The authors interpret their results in terms of a proximity effect. They argue that a good contact with the normal metal depresses the d-wave order parameter near the interface, because this symmetry channel is very unfavorable for a proximity induced order parameter in N. In the presence of a sub-dominant s-symmetry channel in S, that symmetry can then manifest itself near the interface. An interesting observation by Kohen *et al.* (Kohen *et al.*, 2003) is that the excitation gap for the case of a $(d + is)$ order parameter, $\Delta_g = (\Delta_d^2 + \Delta_s^2)^{1/2}$, does scale with T_c , meaning that it retains at the surface its bulk value, although the respective weights of the two components vary with Z from junction to junction.

D. Spin effects

ASJ reflections are profoundly modified at the interface with a ferromagnetic metal. This topic has been recently reviewed by Zutic (Zutic *et al.*, 2004). As the spin polarization increases, the conductance of a Sharvin contact at subgap voltages decreases: spin conservation requires that the ASJ reflected hole must have a spin opposite to that of the incoming electron, a process incompatible with full spin polarization in the ferromagnet (deJong and Beenakker, 1995). This has been verified experimentally (Soulen *et al.*, 1998; Upadhyay *et al.*, 1998). Zutic and Valls (Zutic and O.T.Valls, 1999) and Zutic and Valls (Zutic and O.T.Valls, 2000) have however pointed out that this low bias conductance decrease as the polarization is increased is only a general property for contacts where the Fermi

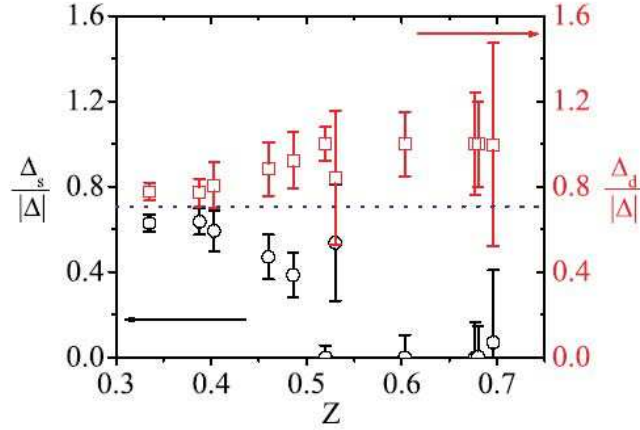


FIG. 24 Variation with the barrier parameter Z of the d-wave component and of the is-wave component at $Au/YBCO$ contacts fitted to the (100) orientation. The is component becomes of the order of the d-wave one for high transparency barriers, suggesting that it is due to a proximity effect. (after Kohen *et al.* 2003).

velocities of both sides are nearly matched. When they are not, the zero-bias conductance may in fact initially rise with the polarization. Care should therefore be exercised when one attempts to extract the value of the polarization from conductance curves. Using for the fit the BTK parameter Z , that does not distinguish between the effect of a dielectric barrier and that of a Fermi velocity mismatch, may not be justified. Chen *et al.* (Chen *et al.*, 2001) have studied transport across the interface between an YBCO layer and a high spin polarized oxide. They conclude that spin polarization tends to diminish the ZBCP feature. There has been recently experimental interest in spin injection from ferromagnets into High- T_c cuprates (Dong *et al.*, 1997; Fu *et al.*, 2002; Vas'ko *et al.*, 1997). Ngai *et al.* (Ngai, 2004) have developed an injection scheme allowing a simultaneous STM measurement, and have shown that spin injection reduces and broadens the ZBCP feature. Theoretical treatment has taken into account the influence of ASJ reflections at the interface, including the effect of d-wave symmetry and particularly that of surface bound states (Kashiwaya *et al.*, 1999; Merrill and Si, 1999; Zhu *et al.*, 1999; Zutic and O.T.Valls, 1999).

Mesoscopic studies of ASJ reflections cover a large field that could be the subject of a review all by itself. We limit ourselves here to a particular situation that is drawing increasing attention, that where two ferromagnetic tips in close proximity are in contact with a superconductor, the distance between them being shorter than the coherence length. Assume that the tips are fully polarized, that they are connected to a busbar and that a difference of potential is applied between this busbar and the superconductor. Then an electron coming from one the ferromagnetic legs cannot be ASJ reflected as a hole in that same leg. It can however be reflected in the other leg, provided the polarizations in the two legs are antiparallel (Deutscher and Feinberg, 2000). As a result, the resistance of the device will depend on the relative magnetic polarizations of the two legs: it will be high if they are parallel, low if they are antiparallel. One can consider the device as some kind of transistor: the resistance can be modified by applying a local magnetic field that can reverse the polarization of one of the two legs. More fundamentally, in the case of antiparallel polarizations, the incoming electron in one leg and the reflected hole in the other one can be considered as two electrons of the same Cooper pair separated in space, a situation that can have interesting implications (Recher and Loss, 2003). The basic prediction of a resistance sensitive to the relative polarizations has just been verified experimentally, as well as the exponential decay of the effect on the scale of the coherence length (Beckmann *et al.*, 2004). The amplitude of the effect is sensitive to the exact geometry and to scattering inside the superconductor (Melin and Feinberg, 2002).

VII. CONCLUSIONS

ASJ reflections are a powerful tool for the study of the nature of electronic excitations in superconductors, determination of energy gap values and studies of the symmetry of the order parameter. Strong ASJ reflections have been observed in all cuprates tested so far, including in the underdoped- pseudogap regime. Because their occurrence implies electron-hole mixing, it follows that the nature of electronic excitations in the cuprates is similar to that in ordinary metals. This is an important result, which can help to discriminate between the predictions of different theoretical HTSC models. From the energy dependence of ASJ reflections, one can infer that the scale of coherent, homogeneous superconductivity is on the order of 20 meV. Pseudogap values substantially exceeding this value may not be related directly to superconductivity, and are apparently characteristic of the anti-node directions. If the pseudogap is a high temperature precursor of superconductivity, it must be strongly momentum dependent. The same holds if it is the manifestation of a competing order. ASJ doping dependence gives indications for the existence of an additional interaction channel, besides the one giving rise to d-wave symmetry. This additional channel becomes stronger as doping is increased beyond optimum doping. ASJ spectroscopy under applied magnetic fields provides a tool for the study of surface currents, including Meissner currents due to an effective Bean-Livingston barrier against vortex penetration, and currents possibly linked to an imaginary component of the order parameter induced by the magnetic field.

Acknowledgments

I am greatly indebted to Philippe Nozieres and to Fabio Pistolesi for numerous illuminating discussions and for giving me access to their unpublished results on Andreev - Saint James reflections in the strong coupling regime. Many thanks are due to Jacques Friedel for his patient explanations on the origin of the pseudogap concept, and to Roger Maynard for many fruitful discussions on ASJ reflections and related topics. Much help from and discussions with Meir Weger, Bernard Raveau and Alex Revcolevschi are gratefully acknowledged. A special thank is due to Amir Kohen and to Roy Beck for providing a number of useful numerical simulations. The major part of this review was prepared while I was a guest at the Institut Laue - Langevin, which I would like to thank for its support. I would also like to thank warmly Efim Kats for his hospitality during this stay, and for many interesting discussions. Finally, I would like to thank Yoram Dagan, Amir Kohen, Roy Beck and Guy Leibovitch of the Tel Aviv team, and Oded Millo and Gad Koren for their many contributions to this work. Support from the Israel Science Foundation, from the Heinrich Hertz - Minerva Center for High Temperature Superconductivity and from the Oren Family Chair for Experimental Solid State Physics is gratefully acknowledged.

References

- Achsaf, N., G. Deutscher, A. Revcolevschi, and M. Okuya, 1996, in *Coherence in high temperature superconductors*, edited by G. Deutscher and A. Revcolevschi (World Scientific), p. 428.
- Alff, L., Y. Krockenberger, B. Welter, M. Schonecke, R. Gross, D. Manske, and M. Naito, 2003, *Nature* **422**, 698.
- Alff, L., H. Takashima, S. Kashiwaya, N. Terada, T. Ito, K. Oka, Y. Tanaka, and M. Koyanagi, 1997, *Physica C* **282-287**, 1485.
- Alloul, H., T. Ohno, and P. Mendels, 1989, *Phys.Rev.B* **63**, 1700.
- Altman, E. and A. Auerbach, 2002, *Phys.Rev.B* **65**, 104508.
- Anderson, P., 1987, *Science* **235**, 1196.
- Andreev, A., 1964, *Zh.Ekperim.i.Teor. Fiz.* **46**, 1823, (Soviet Physics JETP 19, 1228).
- Aprili, M., E. Badica, and L. Greene, 1999, *Phys.Rev.Lett.* **83**, 4630.
- Aubin, H., G. L.H., S. Jian, and D. Hinks, 2002, *Phys.Rev.Lett.* **89**, 177008.
- Bean, C. and J. Livingston, 1968, *Phys.Rev.Lett.* **12**, 14.
- Beck, R., Y. Dagan, A. Milner, A. Gerber, and G. Deutscher, 2004, *Phys.Rev. B* **69**, 1440506.
- Beck, R., A. Kohen, G. Leibovitch, H. Castro, and G. Deutscher, 2003, *J.of Low Temperature Physics* **131**, 451.
- Beckmann, D., H. Weber, and H. Lohneysen, 2004, eprint cond-mat/0404360.
- Benfatto, L., S. Caprata, and C. Castro, 2000, eprint cond-mat/0002250.
- Bernegiv, B., G. Chapline, R. Laughlin, Z. Nazario, and D. Santiago, 2003, eprint cond-mat/0312573.
- Bernhardt, C., C. Niedermayer, and U. *et al.*, 1995, *Phys.Rev.B* **52**, 104881.
- Blonder, G., M. T. M., and T. Klapwijk, 1982, *Phys.Rev.B* **25**, 4515.
- Blonder, G. and M.Tinkham, 1983, *Phys.Rev.B* **27**, 112.
- Bogoliubov, N., 1958, *J.Ekperim.i.Teor.Fiz..(U.S.S.R.)* **34**, 58, (Soviet Physics J.E.T.P. **7**, 41 (1958)); *J.Phys.USSR* **11**, 23 (1947).
- Buchholz, L. and G. Zwirnagl, 1981, *Phys.Rev.B* **23**, 5788.
- Bussieres, J., 1976, *Phys.Lett.* **58A**, 343.
- Caroli, C., P. De-Gennes, and J. Matricon, 1964, *Phys.Lett* **9**, 307.
- Castellani, C., C. di Castro, and M. Grilli, 1997, *Z.Phys.B Condens.Matter* **103**, 137.
- Chen, Q., J. Stajic, A. Tan, and K. Levin, 2004, to be submitted to *Reviews of Modern Physics.*, eprint cond-mat/0404274.
- Chen, Z., A. Biswas, I. uti, T. Wu, S. B. Ogale, R. L. Greene, and T. Venkatesan, 2001, *Phys.Rev.B* **63**, 212508.
- Covington, M., M. Aprili, E. Paraonu, L. Greene, F. Xu, J. Zhu, and C. Mirkin, 1997, *Phys.Rev.Lett.* **79**, 277.
- Dagan, Y. and G. Deutscher, 2001a, *Phys.Rev.Lett.* **87**, 177004.
- Dagan, Y. and G. Deutscher, 2001b, *Phys.Rev.B* **64**, 092509.
- Dagan, Y., A. Kohen, G. Deutscher, and A. Revcolevschi, 2000, *Phys.Rev.B* **61**, 7012.
- Daghero, D., R. Gonelli, G. Ummarino, and V. Stepanov, 2002, eprint cond-mat/0207411.
- De-Gennes, P., 1966, *Superconductivity of metals and alloys* (W.A.Benjamin Inc., New York), p. 137.
- De-Gennes, P. and D. S. James, 1963, *Phys.Letters* **4**, 151.
- deJong, M. J. M. and C. W. J. Beenakker, 1995, *Phys. Rev. Lett.* **74**, 1657.
- Deutscher, G., 1999, *Nature* **397**, 411.
- Deutscher, G. and P. De-Gennes, 1969, in *Superconductivity*, edited by R. Parks (Marcel Dekker Inc., New York), p. 1005.
- Deutscher, G. and D. Feinberg, 2000, *Applied Physics Letters* **76**(4), 487, URL <http://link.aip.org/link/?APL/76/487/1>.
- Deutscher, G. and R. Maynard, 1998, in *Gap symmetry and fluctuations in High Temperature Superconductors*, edited by J. Bok and G. Deutscher (D.Pavuna and S.Wolf Plenum NATO ASI series), volume 371, p. 487.
- Deutscher, G. and P. Nozieres, 1994, *Phys. Rev. B* **50**, 13557.
- D'Gorno, I. and A. Kohen, 1998, unpublished.
- Ding, H., M. Norman, T. Machiku, K. Kadowaki, and J. Giapinzakis, 1996, *Nature* **382**, 51.
- Dong, Z., R. Ramesh, and T. Venkatesan, 1997, *Appl.Phys.Lett.* **71**, 1718.
- Emery, V. and S. Kivelson, 1995, *Nature* **374**, 434.
- Ernst, G., A. Nowack, M. Weger, and D. Schweizer, 1994, *Europhys.Lett.* **25**, 303.
- Fischer, O., C. Renner, and I. M. Aprile, 1998, in *The Gap symmetry and fluctuations in high temperature superconductors*, edited by G. D. J. Bok (D.Pavuna and S.Wolf, Plenum NATO ASI series), volume 371, p. 487.
- Fogelstrom, M., D. Rainer, and J. Sauls, 1997, *Phys.Rev.Lett.* **79**, 281.
- Fogelstrom, M., D. Rainer, and J. Sauls, 2003, eprint cond-mat/0302197.
- Fournier, P., E. Maiser, and R. Greene, 1998, in *The Gap symmetry and fluctuations in high temperature superconductors*, edited by J. Bok, G. D. D. Pavuna, and S. Wolf (Plenum NATO ASI series), volume 371, p. 145.
- Friedberg, R. and T. Lee, 1989, *Phys.Rev.B* **40**, 6745.
- Friedel, J., 1988, *Physica C* **153**, 1610.
- Friedel, J., 1989, *J.Phys.Cond.Matt.* **1**, 7757.
- Friedel, J. and M. Kohmoto, 2002, *Eur.Phys.J.B* **30**, 427.
- Fu, C., Z. Huang, and N.-C. Yeh, 2002, *Phys.Rev.B* **65**, 224516.
- Giaever, I., 1960, *Phys.Rev.Letters* **5**, 147.
- Goll, G., H. Lohneysen, I. Yanson, and L. Taillefer, 1993, *Phys.Rev.Lett.* **70**, 2008.
- Griffin, A. and J. Demers, 1971, *Phys.Rev.B* **4**, 2202.

- Hass, N., G. Deutscher, A. Revcolevschi, and G. Dhalenne, 1994, *J. of Superconductivity* **7**, 763.
- Hass, N., D. Ilzyer, G. Deutscher, G. Desgardin, I. Monot, and M. Weger, 1992, *J. of Superconductivity* **5**, 191, see also Hass, N., D. Ilzyer, G. Deutscher, G. Desgardin, I. Monot and M. Weger (1993) Gap anisotropy and Fermi velocity in oriented $YBa_2Cu_3O_{7-x}$, *Physica C* **209**, 85.
- Hasselbach, K., J. Kirtley, and J. Lejay, 1993, *Physica B* **186-188**, 201.
- Hu, C.-R., 1994, *Phys.Rev.Lett.* **72**, 1526.
- Junod, A., A. Erb, and C. Renner, 1999, *Physica C* **317-318**, 333.
- Kashiwaya, S., Y. Tanaka, and K. *et al.*, 1995, *Phys.Rev.B* **51**, 1350.
- Kashiwaya, S., Y. Tanaka, N. Yoshida, and M. Beasley, 1999, *Phys.Rev.B* **60**, 3572.
- Kleefisch, S., B.Welter, A. Marx, L. Alff, R. Gross, and M. Naito, 2001, *Phys.Rev. B* **63**, R100507.
- Kohen, A., G. Leibovitch, and G. Deutscher, 2003, *Phys. Rev.Lett.* **90**, 207005.
- Krupke, R. and G. Deutscher, 1999, *Phys.Rev.Lett.* **83**, 4634.
- Laughlin, R., 1998, *Phys.Rev.Lett.* **80**, 5188.
- Laughlin, R., 2002, eprint cond-mat/0209269.
- Leggett, A., 1980, in *Modern trends in the theory of condensed matter*, edited by A. Bekalsky and J. Przyspawa (Springer Verlag, Berlin), p. 13.
- Lesueur, J., L. Greene, W. Feldmann, and I. Inam, 1992, *Physica C* **191**, 325.
- Marcenat, C., R. Calemszuk, and A. Carrington, 1996, in *Coherence in high temperature superconductors*, edited by G. Deutscher and A. Revcolevschi (World scientific), p. 101.
- Margaritondo, 1998, in *Gap symmetry and fluctuations in High- T_c superconductors*, edited by J. Bok, G. Deutscher, D. Pavuna, and S. Wolf (Plenum Press), p. 195.
- Marini, M., F. F., and G. Strinati, 1998, *Eur. Phys.J.B* **1**, 151.
- Massida, S., J. Yu, K. Park, and A. Freeman, 1991, *Physica C* **176**, 159.
- McElroy, K., D.-H. Lee, J. E. Hoffman, K. M. Lang, E. W. Hudson, H. Eisaki, S. Uchida, J. Lee, and J. Davis, 2004, eprint cond-mat/0404005.
- McMillan, W. and J.M.Rowell, 1969, in *Superconductivity*, edited by R.D.Parks (Marcel Dekker Inc., New York), p. 561.
- Melin, R. and D. Feinberg, 2002, *Eur. Phys. J. B* **26**, 101.
- Mendelssohn, K. and J. Olsen, 1950, *Phys.Rev.* **80**, 859.
- Merril, R. and Q. Si, 1999, *Phys.Rev.Lett.* **83**, 5326.
- Miyakawa, N., P. Guptasarma, and J. Zasadzinski, 1997, *Phys.Rev.Lett.* **80**, 157.
- Muller, K. A., 2004, *J. of Superconductivity* **17**, 3.
- Ng, T. K. and C. M. Varma, 2004, eprint Cond-mat/0403379.
- Ngai, J., 2004, *Appl.Phys.Lett.* **84**, 1908.
- Nozieres, P. and F. Pistolesi, 1999, *Eur.Phys.J.B.* **10**, 649.
- Nozieres, P. and S. Schmitt-Rink, 1985, *J.Low Temp.Phys.* **59**, 195.
- Pankove, J., 1966, *Phys.Letters* **21**, 406.
- Perali, A., C. Castellani, and C. di Castro *et al.*, 2000, *Phys.Rev.B* **62**, R9295.
- Pistolesi, F., 1998, unpublished.
- Pistolesi, F. and P. Nozieres, 2000, unpublished.
- Pistolesi, F. and G. Strinati, 1996, *Phys.Rev.B* **53**, 15168.
- Pryadko, L., S. Kivelson, and O. Zachar, 2004, *Phys.Rev.Lett.* **92**, 067002.
- Qazilbash, M., A. Biswas, Y. Dagan, R. Ott, and R. Greene, 2003, *Phys.Rev.B* **68**, 024502.
- Racah, D. and G.Deutscher, 1996, *Physica C* **263**, 218.
- Ranninger, J., J. Robin, and M. Eschrig, 1995, *Phys.Rev.Lett.* **74**, 4027.
- Recher, P. and D. Loss, 2003, *Physical Review Letters* **91**(26), 267003 (pages 4), URL <http://link.aps.org/abstract/PRL/v91/e267003>.
- Renner, C., B. Revaz, and J.-Y. G. *et al.*, 1997, *Phys.Rev.Lett.* **80**, 149.
- Sachdev, S., 2000, *Science* **288**, 475.
- Saint-James, D., 1964, *J.de Physique* **25**, 899.
- Sharoni, A., G. Koren, and O. Millo, 2001, *Europhys.Lett.* **54**, 675.
- Sharoni, A., G. Leibovitch, A. Kohen, R. Beck, G. Deutscher, G. Koren, and O. Millo, 2003, *Europhys. Lett.* **62**, 883.
- Sharoni, A., O. Millo, A. Kohen, Y. Dagan, R. Beck, G. Deutscher, and G. Koren, 2002, *Phys. Rev. B* **65**, 134526.
- Sharvin, Y., 1965, *Zh.Ekperim.i.Teor.Fiz.(U.S.S.R.)* **48**, 984, (*Soviet Physics JETP* **21**, 655).
- Sinha, S. and K.-W. Ng, 1998, *Phys.Rev.Lett.* **80**, 1296.
- Skinta, J., M. Kim, T. Lemberger, T. Greibe, and M. Naito, 2002, *Phys.Rev.Lett.* **88**, 207005.
- Soulen, R., J. Byers, J. M. Osofsky, M. S. Nadgorny, B. Ambrose, T. Cheng, S. F. Broussard, P. R. Tanaka, C. T. Nowak, J. Moodera, J. S. Barry, A. Coey, *et al.*, 1998, *Science* **282**(5386), 85, URL <http://www.sciencemag.org/cgi/content/abstract/282/5386/85>.
- Tallon, J. and J. Loram, 2001, *Physica C* **349**, 53.
- Tanaka, Y., 1996, in *Coherence in high temperature superconductors*, edited by G. Deutscher and A. Revcolevschi (World Scientific), p. 393.
- Timusk, T. and B. Statt, 1999, *Rep.Prog.Phys.* **62**, 61.
- Tsuei, C. C. and J. R. Kirtley, 2000a, *Rev.Mod.Phys.* **72**, 969.
- Tsuei, C. C. and J. R. Kirtley, 2000b, *Phys.Rev.Lett.* **85**, 182.

- Uemura, Y. J., 2002, eprint Cond-mat/0212643.
- Upadhyay, S. K., A. Palanisami, R. N. Louie, and R. A. Buhrman, 1998, Phys. Rev. Lett. **81**, 3247.
- Vas'ko, V. A., V. A. Larkin, P. A. Kraus, K. R. Nikolaev, D. E. Grupp, C. A. Nordman, and A. M. Goldman, 1997, Phys.Rev.Lett. **78**, 1134.
- Walker, M. and P. Pairor, 1999, Phys.Rev. B **59**, 1421.
- Wei, J., N.-C. Yeh, D. Garrigas, and M. Strasik, 1998, Phys.Rev.Lett. **81**, 2542.
- Wolf, S., 1971, Ph.D. thesis, Rutgers University.
- Wollman, D., D. van Harlingen, W. Lee, D. Ginsberg, and A. Leggett, 1993, Phys,Rev.Lett. **71**, 2134.
- Yagil, Y., N. Hass, G. Desgardin, and I. Monot, 1995, Physica C **250**, 59.
- Yang, J. and C.-R. Hu, 1994, Phys.Rev.B **50**, 16766.
- Zaitsev, A., 1980, Soviet Physics JETP **51**, 111.
- Zavaritskii, N., 1960, Zh.Ekperim.i.Teor.Fiz. **38**, 1673, (Soviet Physics JETP 38, 1673).
- Zhu, J., B. Friedman, and C. Ting, 1999, Phys. Rev. B **59**, 9558.
- Zutic, I., J. Fabian, and S. das Sarma, 2004, Rev. Mod. Phys. **76**, 323.
- Zutic, I. and O.T.Valls, 1999, Phys. Rev. B **60**, 6320.
- Zutic, I. and O.T.Valls, 2000, Phys. Rev. B **61**, 1555.